1510

Epitaxial Strain Effects and Superconductor-Insulator Transition in Ultrathin $La_{2-x}Sr_xCuO_4$ Films

Thèse présentée à

la Faculté des Sciences de l'Université de Neuchâtel

pour l'obtention du grade de
Docteur ès Sciences

Joël Perret
physicien diplômé
de l'Université de Neuchâtel

Neuchâtel, février 2000

IMPRIMATUR POUR LA THÈSE

Epitaxial strain effects and superconductor-insulator transition in ultrathin $La_{2-x}Sr_xCuO_4$ films

de M. Joël Perret

UNIVERSITÉ DE NEUCHÂTEL

FACULTÉ DES SCIENCES

La Faculté des sciences de l'Université de Neuchâtel sur le rapport des membres du jury,

MM. P. Martinoli (directeur de thèse), H. Beck, Ø. Fischer (Genève), J.-P. Locquet (Rüschlikon) et T. Schneider (Zürich)

autorise l'impression de la présente thèse.

Neuchâtel, le 13 mars 2000

Le doyen:

J.-P. Derendinger

Abstract

This is a study of the $La_{2-x}Sr_xCuO_4$ (referred to hereafter as LSCO) system. It presents the growth of thin films, their structural characterization, and the investigation of their physical properties.

A customized molecular beam epitaxy (MBE) system is used to grow LSCO samples of various composition on $SrTiO_3$ (STO) and $SrLaAlO_4$ (SLAO) substrates. The powerful RF plasma source of atomic oxygen, the sequential deposition as well as a very low deposition rate (less than 0.5 unit cell per minute) allowed us to grow high-quality epitaxial thin films. The sample quality was checked with reflection high-energy electron diffraction (RHEED), X-ray diffraction, and transmission electron microscopy (TEM) measurements.

It is known that the superconducting transition temperature of high-T_c compounds is usually very sensitive to external applied pressure. Part of this thesis is devoted to an investigation of the influence of epitaxial strain (pressure) on the physical properties of ultrathin films. STO and SLAO single crystals can be used to induce tensile and compressive strain, respectively. In both cases the bi-axial pressure is applied along the in-plane directions, leaving the c-axis free to increase or decrease. The main result is a doubling of the critical temperature T_c of the LSCO from 25 K for the bulk material to 49.1 K for a 150 Å thick film under compressive strain. The counterpart of this result, $T_c = 10$ K under tensile strain, is also intriguing. The normal-state transport measurements revealed that insulating behavior is obtained under tensile strain (STO) and metallic behavior under compressive strain (SLAO). These results taught us several things. First, the critical temperature T_c increases as the distance between two adjacent CuO_2 planes increases, ruling out interlayer tunneling theories. Second, a higher T_c is obtained for compounds with the largest Cu-O_{apical} bond length. This general trend is valid for the single and double-layer compounds.

This work was essentially focused on the underdoped regime of the phase diagram (T_c,x), close to the superconductor-to-insulator (SI) transition. Measurements of the in-plane penetration depth $\lambda_{ab}(T)$ of ultrathin LSCO films reveal that, in the extreme underdoped regime, the zero-temperature areal superfluid density $n_s(0) \propto 1/\lambda_{ab}^2(0)$ follows the quantum prediction $n_s(0) \propto T_c$. This observation is interpreted as a clear manifestation of the fundamental role of quantum phase fluctuations in the underdoped quasi-2D regime of the cuprates. An analysis of the data in terms of the Emery-Kivelson model for superconductors with a small superfluid density, where the strength of quantum fluctuations is controlled by the normal-state resistivity ρ of the material, shows that the zero-temperature SI transition of LSCO occurs when the sheet resistance ρ/d of its 2D elementary superconducting unit (of thickness $d_s = 0.66$ nm) is about twice the quantum resistance $R_Q = h/(2e)^2$.

Note: Ce fascicule contient une version réduite de la thèse.
Une version complète peut être obtenue auprès de la bibliothèque principale de l'Université de Neuchâtel.

Published work

- J. Vanacken, L. Trappeniers, G. Teniers, P. Wagner, K. Rosseel, J. Perret, P. Martinoli, J.-P. Locquet, V.V. Moshchalkov and Y. Bruynseraede, *submitted to Physica C* (1999).

- J.-P. Locquet, J. Perret, J. Fompeyrine, E. Mächler, J.W. Seo and G. Van Tendeloo, "Doubling the critical temperature of $La_{1.9}Sr_{0.1}CuO_4$ using epitaxial strain", *Nature* **394**, pp. 453-456 (1998).

- J. Perret, J. Fompeyrine, J. W. Seo, E. Mächler, Ø. Fischer, P. Martinolsi and J.-P. Locquet, "Critical temperature enhancement by means of substrate-induced pressure", Superconducting and Related Oxides: Physics and Nanoengineering III, edited by D. Pavuna and I. Bozovic, SPIE Proc. 3481, pp. 310-316, San Diego, 1998.

- J. W. Seo, J. Perret, J. Fompeyrine, G. Van Tendeloo and J.-P. Locquet, "Microstructural investigation of $La_{1.9}Sr_{0.1}CuO_4$ thin film grown by MBE", Superconducting and Related Oxides: Physics and Nanoengineering III, edited by D. Pavuna and I. Bozovic, SPIE Proc. 3481, pp. 300-309, San Diego, 1998.

- J. Fompeyrine, R. Berger, Ch. Gerber, J. Perret, J. W. Seo and J.-P. Locquet, "Local determination of the terminating layer of $SrTiO_3$", Superconducting and Related Oxides: Physics and Nanoengineering III, edited by D. Pavuna and I. Bozovic, SPIE Proc. 3481, pp. 274-279, San Diego, 1998.

- J.-P. Locquet, J. Perret, J. W. Seo and J. Fompeyrine, "Changes of T_c under epitaxial strain: Implications for the mechanism of superconductivity", Superconducting and Related Oxides: Physics and Nanoengineering III, edited by D. Pavuna and I. Bozovic, SPIE Proc. 3481, pp. 248-264, San Diego, 1998.

- J.W. Seo, J. Perret, J. Fompeyrine, J.-P. Locquet and G. Van Tendeloo, "$La_{1.9}Sr_{0.1}CuO_4$ thin films grown under compressive strain: a TEM study", *in preparation* (1999).

- J. Fompeyrine, R. Berger, H.P. Lang, J. Perret, E. Mächler, Ch. Gerber and J.-P. Locquet, "Local determination of the stacking sequence of layered materials", *Appl. Phys. Lett.* **72**, pp. 1697-1699 (1998).

- J.W. Seo, J. Perret, J. Fompeyrine, J.-P. Locquet and G. Van Tendeloo, "Microstructural investigation of a La1.9Sr0.1CuO4 thin film grown by MBE under a large compressive strain", Proc. of 14th ICEM Conference, Cancún, (1998).

• E.J. Williams, A. Daridon, F. Arrouy, J. Perret, Y. Jaccard, J.-P. Locquet, E. Mächler, H. Siegenthaler, P. Martinoli and Ø. Fischer, "Transmission electron microscopy investigations of defects in molecular beam epitaxy-grown oxide films", *Journal of Alloys and Compounds* **251**, pp. 11-14 (1997).

Doubling the critical temperature of $La_{1.9}Sr_{0.1}CuO_4$ using epitaxial strain

J.-P. Locquet*, J. Perret*†, J. Fompeyrine*‡, E. Mächler*, J. W. Seo*† & G. Van Tendeloo§

** IBM Research Division, Zurich Research Laboratory, CH-8803 Rüschlikon, Switzerland*

† Institut de Physique, Université de Neuchâtel, CH-2000 Neuchâtel, Switzerland

‡ Institute of Inorganic Chemistry, University of Bern, CH-3012 Bern, Switzerland

§ EMAT, RUCA, University of Antwerp, B-2020 Antwerpen, Belgium

The discovery[1] of high-temperature superconductivity in copper oxides raised the possibility that superconductivity could be achieved at room temperature. But since 1993, when a critical temperature (T_c) of 133 K was observed in the $HgBa_2Ca_2Cu_3O_{8+\delta}$ (ref. 2), no further progress has been made in raising the critical temperature through material design. It has been shown, however, that the application of hydrostatic pressure can raise T_c—up to ~164 K in the case of $HgBa_2Ca_2Cu_3O_{8+\delta}$ (ref. 3). Here we show, by analysing the uniaxial strain and pressure derivatives of T_c, that compressive epitaxial strain in thin films of copper oxide superconductors could in principle generate much larger increases in the critical temperature than obtained by comparable hydrostatic pressures. We demonstrate the experimental feasibility of this approach for the compound $La_{1.9}Sr_{0.1}CuO_4$, where we obtain a critical temperature of 49 K in strained single-crystal thin films—roughly double the bulk value of 25 K. Furthermore, the resistive behaviour at low temperatures (but above T_c) of the strained samples changes markedly, going from insulating to metallic.

A high-pressure state in thin films can be induced by using epitaxial strain[4,5], but only moderate increases of T_c have been reported (+15%; refs 6, 7). Here we first re-examine published uniaxial pressure or strain derivatives of T_c, and predict that under compressive epitaxial strain a much larger increase in T_c must be

Table 1 Uniaxial pressure and strain derivatives with estimated possible increase of T_c

Compound	$\frac{\delta T_c}{\delta \epsilon_{ab}}$ (K)	$\frac{\delta T_c}{\delta \epsilon_c}$ (K)	$\Delta T_c^{\epsilon*}$ (K)	$\frac{\delta T_c}{\delta P_{ab}}$ (K GPa^{-1})	$\frac{\delta T_c}{\delta P_c}$ (K GPa^{-1})	ΔT_c^{P}† (K)
$La_{1.91}Sr_{0.09}CuO_4$ (ref. 8)	284	−851	10	3.2	−6.6	32
$La_{1.9}Sr_{0.10}CuO_4$ (ref. 9)	375	−2,440	22	6.5	−13.8	65
$YBa_2Cu_3O_7$ (ref. 10)				−0.05	−0.3	−0.5
$YBa_2Cu_3O_7$ (ref. 11)				0.15	~0	1.5
$YBa_2Cu_3O_7$ (ref. 5)				0.5	–	5
$GdBa_2Cu_3O_{7-\delta}$ (ref. 4)	−31	239	−1.2			
$Bi_2Sr_2CaCu_2O_8$ (ref. 12)				1.8	−2.8	18
$Bi_2Sr_2CaCu_2O_8$ (ref. 13)				1.3	−0.8	13
$(Bi,Pb)_2Sr_2CaCu_2O_8$ (ref. 14)				10.0	−18.5	100
$(Bi,Pb)_2Sr_2Ca_2Cu_3O_{10}$ (ref. 14)				6.2	−18.5	62

Values are shown for various compounds. For orthorhombic compounds, values along the *a* and *b* axes have been averaged.
* Estimated change in T_c for $\epsilon_{ab} = -\epsilon_c = 0.7\%$.
† Estimated change in T_c for $\Delta P = 5$ GPa.

possible. We then apply this idea to an underdoped $La_{2-x}Sr_xCuO_4$ (referred to here as '214', with $x = 0.10$) compound, which has a bulk T_c of 25 K.

The pressure (P) and strain ($\epsilon = [d_{bulk} - d_{strained}]/d_{bulk}$, with d a lattice parameter) dependence of T_c for a tetragonal unit cell contains an in-plane (ab) and an out-of-plane (c) term, and is written as follows:

$$T_c = T_c(0) + 2\frac{\delta T_c}{\delta P_{ab}}P + \frac{\delta T_c}{\delta P_c}P = T_c(0) + 2\frac{\delta T_c}{\delta \epsilon_{ab}}\epsilon_{ab} + \frac{\delta T_c}{\delta \epsilon_c}\epsilon_c \quad (1)$$

Table 1 summarizes values of the uniaxial pressure and strain coefficients[8–14]. For most systems, the in-plane and out-of-plane T_c derivatives have opposite signs. Under hydrostatic pressure both terms nearly cancel, leading to a small increase of T_c (refs 15, 16). But under epitaxial growth conditions, ϵ_{ab} and ϵ_c normally have opposite signs (although this is not always the case[17]), and both terms add up to increase (compressive, $\epsilon_{ab} > 0$) or decrease (tensile, $\epsilon_{ab} < 0$) T_c.

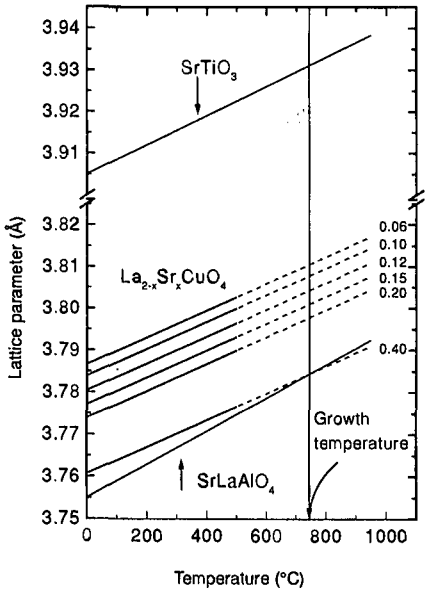

Figure 1 Extrapolated in-plane lattice parameters as a function of temperature. Values are shown for different Sr concentrations of the '214' compound ($La_{2-x}Sr_xCuO_4$, $\alpha = 8.5 \times 10^{-6}\,K^{-1}$) as well as for the SLAO ($SrLaAlO_4$, $\alpha = 10.5 \times 10^{-6}\,K^{-1}$) and STO ($SrTiO_3$, $\alpha = 9 \times 10^{-6}\,K^{-1}$) substrates. Above 500 °C, α_{214} has not been reported. The reflection high-energy electron diffraction data give only relative measurements, but indicate that at 750 °C growth is compressive for $x \leq 0.12$.

To increase T_c significantly, a large amount of compressive strain must be induced. This requires (1) the choice of a suitable system and substrate combination ('214' and $SrLaAlO_4$, referred to here as 'SLAO', with $a = 3.754$ Å); (2) a defect-free growth process (block-by-block molecular beam epitaxy[18]), and (3) an optimal thickness (10–15 nm). This thickness is a compromise between avoiding the nucleation of misfit dislocations and minimizing the T_c reduction observed for ultrathin films[19,20]. Indeed, dislocations appear when a critical thickness h_c has been exceeded[21]; h_c decreases with increasing mismatch, suggesting that a large strain requires very thin films. Such thin (15-nm) '214' films were grown simultaneously on SLAO and $SrTiO_3$ (referred to here as 'STO' with $a = 3.905$ Å, tensile strain) by block-by-block molecular beam epitaxy[18,22] at 750 °C, where a sequence of two monolayers of (La,Sr)–O followed by one monolayer of Cu–O is repeated. High-quality thin films can thus be prepared, and strain-relaxation processes related to the incorporation of defects can be minimized.

Precise estimates of ϵ demand values for the thermal expansion coefficients α of '214' and SLAO. Unfortunately, α_{214} is not known above 500 °C. In Fig. 1, $\alpha_{214} = 8.5 \times 10^{-6}\,K^{-1}$ (ref. 23) and $\alpha_{SLAO} = 10.5 \times 10^{-6}\,K^{-1}$ were used, and compressive strain is predicted at the growth temperature for all '214' compounds with $x \leq 0.4$. However, measurements of ϵ_{ab} during growth using reflection high-energy electron diffraction[22] revealed compressive strain

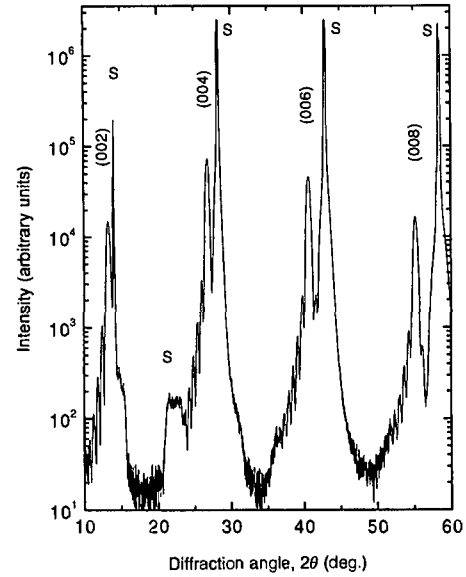

Figure 2 Measured X-ray diffraction pattern of the 12-unit-cell-thick '214' film on SLAO. Besides the substrate peaks indicated by S, only the '214' (00*l*) peaks with their finite-size oscillations are observed. The presence of these finite-size oscillations suggests a film roughness of ±(1–2) unit cells.

only up to $x = 0.12$. This discrepancy might be related to a smaller α_{214} at high temperatures or to the presence of an interface layer[24]. In any case, a large compressive strain requires $x < 0.12$.

The θ–2θ X-ray diffraction pattern of the film grown on SLAO reveals (00l) peaks and finite-size oscillations (Fig. 2). From this and measurements taken around the (107), (109) and (1011) reflections, the lattice parameters $c = 13.31 \pm 0.01$ Å and $a = 3.76 \pm 0.02$ Å were determined (bulk compound[25]: 13.212 and 3.784 Å, respectively) leading to $\epsilon_{ab} = 0.63\%$, $\epsilon_c = -0.76\%$. For the film grown on STO, similar measurements yield $\epsilon_{ab} = -0.54\%$, $\epsilon_c = 0.35\%$. Preliminary X-ray refinements of these data using a modified Suprex[26] program yield a change of the distance between two CuO_2 planes from 6.61 Å (bulk) to 6.65 Å (SLAO) and 6.59 Å (STO). The cross-section, high-resolution transmission electron microscopy image (Fig. 3) of the film grown on SLAO confirms the low defect density in the sample. The film–substrate interface, indicated by arrows, has steps that are one-half of a unit cell high. Despite these steps, perfect continuity of the first '214' layer was obtained, and no defects were observed. On the basis of image simulations (see Fig. 3 inset), the stacking sequence of the interface can be described as LaO–LaO–AlO_2–LaO–CuO_2–LaO–LaO; that is, there is an intermediate La_2CuAlO_6 layer at the interface. In Fig. 3, the white dots in the film and substrate correspond to Cu and Al columns, respectively. By taking the Al–Al distance as a standard, the distances between two CuO_2 planes are obtained directly from lattice fringe spacing refinements, namely 6.63 Å (SLAO) and 6.57 Å (STO). A few misfit dislocations only were found in plan-view samples with an average distance of 200 nm. These have an average length of 150 nm and Burgers vectors of $\mathbf{b} = \langle 100 \rangle$ and $\langle 110 \rangle$. Their presence suggests that the film has nevertheless partially relaxed; thinner films might allow us to increase the strain further.

The values of ϵ determined above, together with the $\delta T_c/\delta\epsilon$ coefficients of Table 1 and the phenomenological equation (1), suggest a substantial change of T_c. Measurements of the resistivity versus temperature $\rho(T)$ (Fig. 4) indeed reveal that the film grown under compressive strain has a T_c of 49.1 K, while the film grown under tensile strain has a T_c of 10 K. Compared with the T_c of the bulk compound[27] (25 K, see dotted line in Fig. 4), these values represent a spectacular increase and decrease, respectively. Such large changes have not been achieved for bulk '214', not even under the highest hydrostatic or uniaxial pressure used up to now.

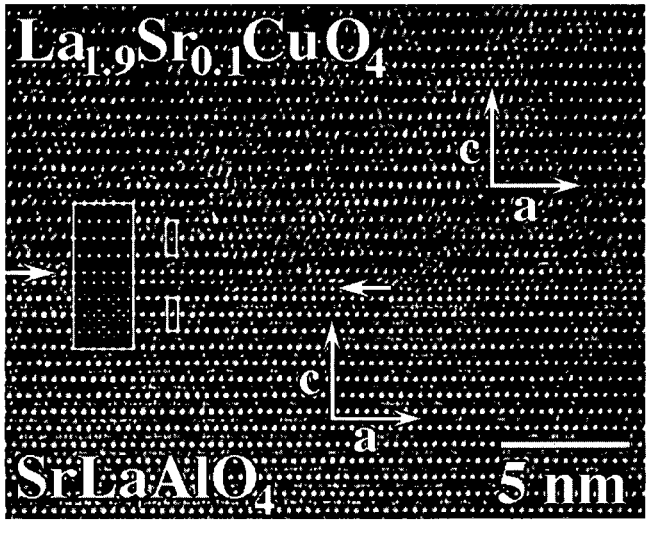

Figure 3 Cross-section, high-resolution electron-microscopy image of the '214' film on SLAO. On the basis of image simulations, the white dots in the film and substrate can be correlated with Cu and Al columns, respectively. The unit cells are indicated by the small white rectangles. The inset shows the simulated image of the interface structure with the stacking sequence LaO-LaO-AlO_2-LaO-CuO_2-LaO-LaO.

At low temperatures ($T < 100$ K), another significant but unexpected change occurs. Compared to the resistive behaviour of the bulk compound (as shown by the $\rho(T)$ curve), the film grown under tensile strain shows a large upturn in this curve as temperature is reduced, before the onset of superconductivity. Such a behaviour has been observed for heavily underdoped '214' compounds ($x \approx 0.06$; ref. 27). On the other hand, the film grown under compressive strain shows a metallic and linear $\rho(T)$, which is usually observed for optimally doped compounds ($x \approx 0.16$; ref. 27). However, we emphasize that in both cases the overall $\rho(T)$ behaviour remains very different from that of typical underdoped or optimally doped samples. For instances, the ratio $\rho(300\,\mathrm{K})/\rho(50\,\mathrm{K})$ for the film on SLAO is ~8, compared with ~4 for the best optimally doped bulk samples[27]. Moreover, at relatively high temperatures (270 K), a change of slope $\delta\rho/\delta T$ occurs for the film on SLAO, towards a value typically observed above the 'pseudogap' temperature T^* (see dashed line in Fig. 4). For the bulk compound, on the other hand, such a change of slope occurs at $T^* \approx 600$ K (ref. 28); that is, under compressive strain T^* is reduced by a factor of two. Hence, these data suggest that in addition to causing a substantial increase of T_c, strain also significantly modifies the normal-state properties.

These changes could partially be explained by variations of the carrier density n. Indeed as n increases, an insulator-to-metal transition is observed[27]. A correlation between an increasing T_c and decreasing T^* as n becomes larger is commonly reported for other copper oxides[29]. However, a rough estimate using the values of $\rho(300\,\mathrm{K})$ indicates that these variations are not larger than ±10%. This certainly cannot explain the observed T_c value of 49 K, which is significantly higher than the maximum observed in the bulk '214' system (37 K for $x = 0.16$).

These results give rise to two fundamental questions. First, can the T_c of other compounds be increased? Table 1 shows that under compressive strain ($P = 5$ GPa or $\epsilon_{ab} = -\epsilon_c = 0.7\%$), significant increases can be expected for some compounds. Unfortunately the uniaxial T_c derivatives for the Tl and Hg compounds are not yet available. Second, how do these observations change our understanding of superconductivity in copper oxides? If the changes in n

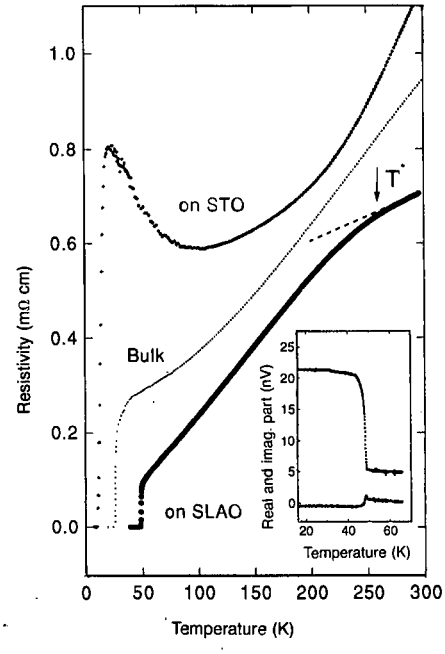

Figure 4 Resistivity versus temperature for the two films grown simultaneously and for the bulk $x = 0.10$ sample[26]. Data were obtained using a four-point method. Inset, Real and imaginary parts of the a.c. susceptibility of the film on SLAO, which reveals a sharp, single-phase transition $\Delta T_c = 0.7$ K; the transition width of the film on STO is $\Delta T_c = 4$ K.

amount to ±10%, this would result in a total T_c variation of 7 K in the bulk phase diagram. In strained films a total variation of ~40 K is observed, together with a drastic change in T^*. Hence, the lattice deformations associated with the strain fundamentally modify the energy scales, leading to the formation and condensation of the superconducting pairs. As the pair formation strongly influences the spin and charge excitation spectrum of the normal state, $\rho(T)$ and the metal–insulator transition are also considerably modified. Further work to identify and quantify the subtle lattice deformations responsible for these changes needs to be done. In any case, the data reported here emphasize that T_c increases as the distance between consecutive CuO_2 planes increases, in contradiction of a recent theoretical prediction[30]. Our data also show that adjustment of the epitaxial strain offers a unique way to increase T_c and to reveal the fundamental role played by the interlayer coupling. □

Received 13 March; accepted 27 May 1998.

1. Bednorz, J. G. & Müller, K. A. Possible high T_c superconductivity in the Ba–La–Cu–O system. *Z. Phys. B* **64**, 189–193 (1986).
2. Schilling, A., Cantoni, M., Guo, J. D. & Ott, H. R. Superconductivity above 130 K in the Hg–Ba–Ca–Cu–O system. *Nature* **362**, 56–58 (1993).
3. Gao, L. *et al.* Superconductivity up to 164 K in $HgBa_2Ca_{m-1}Cu_mO_{2m+2+\delta}$ (m = 1, 2 and 3) under quasihydrostatic pressures. *Phys. Rev. B* **50**, 4260–4263 (1994).
4. Bud'ko, S. L., Guimpel, J., Nakamura, O., Maple, M. B. & Schuller, I. K. Uniaxial pressure dependence of the superconducting critical temperature in $RBa_2Cu_3O_{7-\delta}$ high T_c oxides. *Phys. Rev. B* **46**, 1257–1260 (1992).
5. Belenky, G. L. *et al.* Effect of stress along the *ab* plane on the J_c and T_c of $YBa_2Cu_3O_7$ thin films. *Phys. Rev. B* **44**, 10117–10120 (1991).
6. Sato, H. & Naito, M. Increase in the superconducting transition temperature hy anisotropic strain effect in (001) $La_{1.85}Sr_{0.15}CuO_4$ thin films on $LaSrAlO_4$ substrates. *Physica C* **274**, 221–226 (1997).
7. Locquet, J.-P. & Williams, E. J. Epitaxially induced defects in Sr- and O-doped La_2CuO_4 thin films grown hy MBE: implications for transport properties. *Acta Polonica A* **92**, 69–84 (1997).
8. Nohara, M. *et al.* Unconventional lattice stiffening in superconducting $La_{2-x}Sr_xCuO_4$ single crystals. *Phys. Rev. B* **52**, 570–580 (1995).
9. Gugenherger, F. *et al.* Uniaxial pressure dependence of T_c from high resolution dilatometry of untwinned $La_{2-x}Sr_xCuO_4$ single crystals. *Phys. Rev. B* **49**, 13137–13142 (1994).
10. Welp, U. *et al.* Effect of uniaxial stress on the superconducting transition in $YBa_2Cu_3O_7$. *Phys. Rev. Lett.* **69**, 2130–2133 (1992).
11. Meingast, C. *et al.* Large *a*–*b* anisotropy of the expansivity anomaly at T_c in untwinned $YBa_2Cu_{7-\delta}$. *Phys. Rev. Lett.* **67**, 1634–1637 (1991).
12. Meingast, C., Junod, A. & Walker, E. Superconducting fluctuations and uniaxial pressure dependence of T_c of a $Bi_2Sr_2CaCu_2O_{8+x}$ single crystal from high resolution thermal expansion. *Physica C* **272**, 106–114 (1996).
13. Fukamachi, K. *et al.* in *Advances in Superconductivity* Vol. VII (eds Yamafuji, K. & Morishita, T.) 225–228 (Springer, Tokyo, 1995).
14. Chen, X., Tessema, G. X. & Skove, M. J. Effects of elastic stress on the resistivity and T_c of $(Bi,Pb)_2Sr_2Ca_{n-1}Cu_nO_x$. *Physica C* **181**, 340–344 (1991).
15. Tanahashi, N. *et al.* The strontium content dependence of pressure effect in $(La_{1-x}Sr_x)_2CuO_4$. *Jpn J. Appl. Phys.* **28**, L762–L765 (1989).
16. Yamada, N. & Ido, M. Pressure effects on superconductivity and structural phase transitions in $La_{2-x}M_xCuO_4$ (M = Ba, Sr). *Physica C* **203**, 240–246 (1992).
17. Fartash, A., Grimsditch, M., Fullerton, E. E. & Schuller, Ivan K. Breakdown of Poisson's effect in Nb/Cu superlattices. *Phys. Rev. B* **47**, 12813–12819 (1993).
18. Locquet, J.-P. & Mächler, E. Block-hy-block deposition of complex oxide films. *Mater. Res. Soc. Bull.* **19**, 39–43 (1994).
19. Triscone, J.-M. *et al.* $YBa_2Cu_3O_7/PrBa_2Cu_3O_7$ superlattices: Properties of ultrathin superconducting layers separated hy insulating layers. *Phys. Rev. Lett.* **64**, 804–807 (1990).
20. Terashima, T. *et al.* Superconductivity of one-unit-cell thick $YBa_2Cu_3O_7$ thin film. *Phys. Rev. Lett.* **67**, 1362–1365 (1991).
21. Matthews, J. W. & Blakeslee, A. E. Defects in epitaxial multilayers. *J. Cryst. Growth* **27**, 118–125 (1994).
22. Locquet, J.-P. *et al.* Variation of the in-plane penetration depth λ_{ab} as a function of doping in $La_{2-x}Sr_xCuO_{4\pm\delta}$ thin films on $SrTiO_3$: implications for the overdoped state. *Phys. Rev. B* **54**, 7481–7488 (1996).
23. Tresse, F. *Cristallochimie de Quelques Oxides des Éléments de Transition: Influence de la présence d'oxygène et de Substitutions Cationiques sur la Supraconduction* Thesis, Univ. Bordeaux (1990).
24. Hojczyk, R., Jia, C.-L., Poppe, U. & Urban, K. New insulating materials for high T_c superconductor device applications. *Physica C* **282–287**, 731–732 (1997).
25. Radaelli, P. G. *et al.* Structural and superconducting properties of $La_{2-x}Sr_xCuO_4$ as a function of Sr content. *Phys. Rev. B* **49**, 4163–4175 (1994).
26. Fullerton, E. E., Schuller, I. K., Vanderstraeten, H. & Bruynseraede, Y. Structural refinements from x-ray diffraction. *Phys. Rev. B* **45**, 9292–9310 (1992).
27. Kimura, T. *et al.* In-plane and out-of-plane magnetoresistance in $La_{2-x}Sr_xCuO_4$ single crystals. *Phys. Rev. B* **53**, 8733–8742 (1996).
28. Nakano, T. *et al.* Magnetic properties and electronic conduction of superconducting $La_{2-x}Sr_xCuO_4$. *Phys. Rev. B* **49**, 16000–16008 (1994).
29. Williams, G. V. M., Tallon, J. L., Haines, E. M., Michalak, R. & Dupree, R. NMR evidence for a d-wave normal state pseudogap. *Phys. Rev. Lett.* **78**, 721–724 (1997).
30. Anderson, P. W. *The Theory of Superconductivity in the High T_c Cuprate Superconductors* (Princeton Univ. Press, 1997); C-axis electrodynamics as evidence for the interlayer theory of high temperature superconductivity. *Science* **279**, 1196–1198 (1998).

Acknowledgements. We thank Y. Jaccard, F. Arrouy and E. J. Williams for contributions in the initial phase of this project; P. Martinoli, Ø. Fischer, J.-M. Triscone, J. G. Bednorz and C. Rossel for discussions; and C. Voisard and T. Maeder for the thermal expansion measurements. This work was supported by the Swiss National Science Foundation, the Swiss Priority Project "Minast", and the Belgian UIAP 4/10.

Correspondence and requests for materials should be addressed to J.-P.L. (e-mail: loc@zurich.ibm.com).

Local determination of the stacking sequence of layered materials

J. Fompeyrine,[a] R. Berger,[b] H. P. Lang,[b] J. Perret,[c] E. Mächler, Ch. Gerber, and J.-P. Locquet[d]
IBM Research Division, Zurich Research Laboratory, CH–8803 Rüschlikon, Switzerland

(Received 27 October 1997; accepted for publication 9 February 1998)

The ability to modify the stacking sequence of ultrathin films offers a unique way to change either the interaction strength or the doping, but demands a careful control of each atomic monolayer. Progress is hampered by the lack of a direct method that allows differentiation on a local scale between the various terminating layers of a crystal. Here, the combination of a vacuum annealing process and friction force microscopy reveals this local distinction on a $SrTiO_3$ surface. Using the friction contrast, we find how the terminating layer of a single crystal profoundly influences the terrace edge structure. © *1998 American Institute of Physics.* [S0003-6951(98)01914-7]

In recent years, great progress has been made in the synthesis of novel layered oxides with properties such as high-T_c superconductivity,[1] colossal magnetoresistance,[2] and fatigue-free ferroelectricity.[3] These exceptional properties arise in part due to the spatial separation of the layer containing the charge reservoir and the layer responsible for the relevant interaction such as magnetic coupling or electric polarization. Solid-state synthesis is constrained within boundaries defined by thermodynamic and kinetic rules, including the limited doping range over which properties can be tuned. Thin-film deposition techniques allow these limits to be shifted, as illustrated by the sandwiching of various compounds in superlattices,[4] so far without significantly improving their properties. However, by completely removing periodicity and symmetry along one axis, the properties of a one-unit-cell (UC) film can be massively modified. Contrary to the bulk compounds, in which the effect of each charge reservoir or interaction layer is divided between the layers below and above, adding a single monolayer to such a film can boost either the relevant interaction or the doping. Unfortunately, progress in this field has been hampered by the lack of a nondestructive method allowing a direct local determination of the stacking sequence, including the additional terminating layer (TL).

One specific example of tailoring the doping beyond the bulk limit by adding (or removing) one TL is given, related to superconductivity in a one-UC film of $YBa_2Cu_3O_{7-\delta}$ "123."[5–9] Examples where the interaction strength is modified can be constructed following similar principles. The "123" UC contains two "interaction" layers and *one charge reservoir*. Two stacks, derived from the "123" UC, are shown in Fig. 1 on a $SrTiO_3$ substrate (STO). Stack (a) contains only two "interaction" layers (the CuO_2 planes), whereas stack (b) contains two "interaction" layers plus *two charge reservoirs* (top and bottom CuO plane) and hence could have an increased T_c. These stacks can be grown on STO, but they occur simultaneously with two different "123" stacks[10] for the following reasons. First, the two different TL of STO (TiO_2 and SrO, Fig. 1) impose different starting layers, namely BaO and CuO, respectively.[11] Second, the thermodynamics during film growth allow two stable TL layers to form (the CuO and the BaO layer).[12–16]

This is a general observation for layered compounds: one particular interlayer bond is the weakest and the structure can be cleaved there, leaving two stable configurations on opposite sides of the cleavage plane.[16] In this case, the weakest bond links precisely the BaO plane to the CuO plane. To correlate a measured property with a specific stack requires two important steps: (i) to prepare a substrate with a unique and known TL contrary to the observed mixture[17–20] and (ii) to identify the TL of the dominant stack on the film surface. Critical to both steps is a *direct procedure to check on a local scale the presence, distribution, and nature of the different TL.* In this report such a procedure is presented for STO.

The STO substrates were etched and annealed at $\simeq 1000$ °C in O_2 for a few hours by the manufacturer.[21] They were analyzed here with a scanning force microscope (SFM)[22] after having been annealed in vacuum (10^{-7} Torr) for about 1 h at various temperatures T_a. The same set of experiments has been repeated several times, using different cantilevers for each set of experiments. Hence, tip parameters such as contamination, shape, and roughness can be ruled out, although it is indeed possible to determine them using a systematic method.[23] The SFM topography image [Fig. 2(a)] shows a 0.7-μm^2 region. A systematic analysis of the height differences between the terraces [Fig. 2(c)] reveals $(n+\frac{1}{2})$ UC steps (n integer) and hence *the presence* of two TL as observed previously.[24] The simultaneously recorded friction force microscopy (FFM) image [Fig. 2(b)] reveals a friction contrast (for $T_a \geq 600$ °C) observed for the first time on such a surface.[25] The analysis along the dashed lines [Fig. 2(c)] indicates that a change of contrast occurs only when a $(n+\frac{1}{2})$ UC step — and thus a change of TL — is involved. Hence, Fig. 2(b) reveals *the lateral distribution* of the TL. What is the origin of the friction contrast? The main effect of vacuum annealing on STO is a loss of oxygen from the TiO_2 layer at high values of T_a,[26] eventually leading to a

[a]Also at: Institute of Inorganic Chemistry, University of Bern, CH-3012 Bern, Switzerland.
[b]Also at: Institute of Physics, University of Basel, CH-4056 Basel, Switzerland.
[c]Also at: Institut de Physique, Université de Neuchâtel, Switzerland.
[d]Corresponding author: Electronic mail: loc@zurich.ibm.com

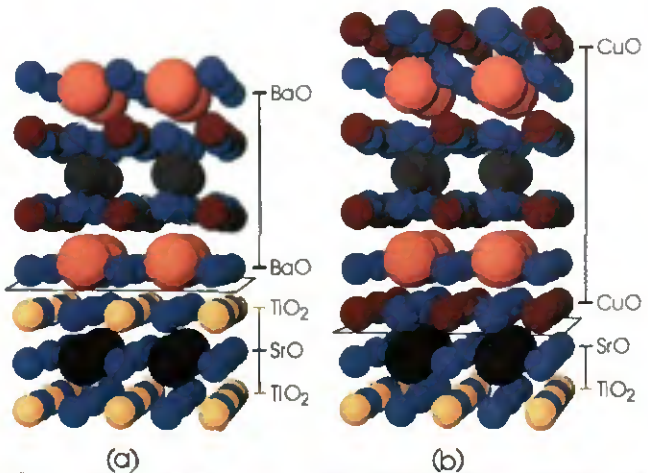

FIG. 1. Atomic model of two "123"-derived stacking sequences on STO(001): (a) a "122" stack with two interaction layers, grown on a TiO_2-terminated surface (one-UC STO shown); (b) a "124" stack with two interaction layers plus two charge reservoirs (top and bottom layer) grown on a SrO-terminated surface ($\frac{1}{2}$-UC STO shown). Color code: Cu (red), Y (green), Ba (orange), Ti (yellow), Sr (blue), O (light blue); the substrate-film interfaces are indicated by planes. In these "123"-derived stacks, the charge reservoir corresponds to the top and bottom CuO layers (b), whereas the antiferromagnetic interaction is confined to the two central CuO_2 planes.

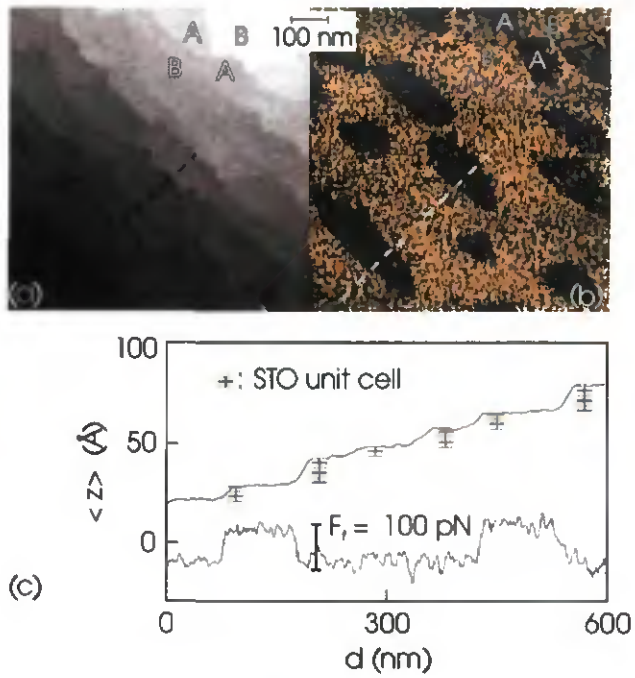

FIG. 2. Simultaneous SFM images of the same surface area of STO, $T_a = 800$ °C, reveal (a) a map of the topography and (b) the lateral forces. The normal loading applied between the tip and the sample for imaging was estimated to be $F_n = 17$ nN. The topography data were corrected by fitting a plane along a single terrace to align the terraces horizontally. This allows us to analyze their vertical separations in detail. A profile, outlined by a dashed line perpendicular to six steps, is plotted in (c), beneath which the corresponding friction contrast along the same line is drawn. The lateral force contrast reveals two values, which correspond to a friction contrast of 90 ±20 pN. Only when the friction contrast changes from one terrace to another are they separated vertically by a $(n+\frac{1}{2})$-UC step. The TL of STO is schematically outlined and correlated with the colors according to the atomic model in Fig. 1. Higher friction — the blue area in (b) — corresponds to the SrO TL, and lower friction — the yellow area — corresponds to the TiO_2 TL ($\mu_{SrO}/\mu_{TiO_2} \simeq 3/2$). The friction contrast images clearly reveal a map of the lateral distribution of TLs.

vacancy-induced superstructure.[27] Using medium-energy ion scattering,[28] a high oxygen desorption was measured above 500 °C, coinciding with the observed increase in friction contrast (μ_A/μ_B) from 1 to 3/2, as derived from the FFM data. A study on other oxide surfaces[29] revealed that friction decreases as the bond density between tip and surface oxygen atoms decreases, suggesting that the low friction surface has the TiO_2 TL. This agrees with the substrate preparation process of the manufacturer, which preferentially removes SrO,[21] leaving TiO_2 as the dominant TL.

Having *identified* the TL locally, the topography in Fig. 2 can be analyzed further and reveals two types of terraces (A and B) with different edges (A: rounded, B: indented). The contours of these edges are outlined in Fig. 3. The TiO_2-terminated terrace edges meander along [100] and [010] for typically 10–50 nm, whereas the SrO-terminated terraces edges are curved with a radius of ≃70–300 nm. Hence we have discovered how the TL determines the terrace edge structure, even for edges several UC high. Whether this is due to a TL-specific surface mobility and diffusion (kinetics) of the migrating species or to differences in line tension and equilibrium shape (thermodynamics) is not clear.

The substrate preparation can now be optimized by etching[20] plus annealing,[24] while the surface composition is determined according to our procedure. Once substrates are available with only one TL, "123" ultrathin stacks can be grown. To identify the distribution and nature of the different stacks, the same procedure can be repeated. In our specific example, only the CuO plane easily loses oxygen upon vacuum annealing.[30] This is again a general observation for layered compounds: the TL often coincides with layers containing atoms whose valence state is reversibly changed by a loss or gain of oxygen (Ti and Cu here). To control artificially the TL of such materials requires, first, the use of a deposition system with an atomic layer control and, second, a knowledge of defect chemistry for each material in order to choose those TL that are likely to be stabilized. On a surface

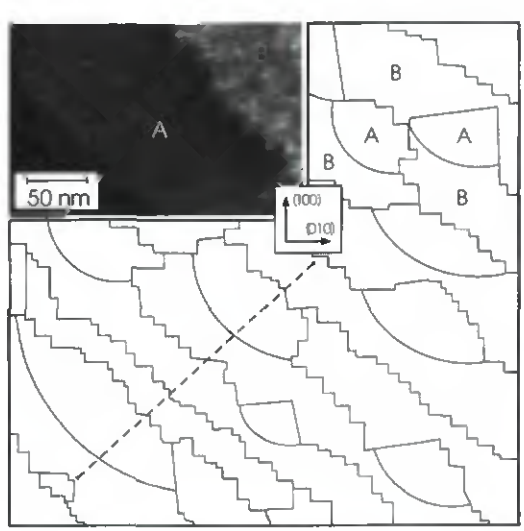

FIG. 3. The contours of the edges based on the SFM and FFM data in Fig. 2 are outlined for clarity. The terraces (A and B) with different shapes of step edges are clearly distinguishable. The inset shows the topography at higher magnification, revealing details of the two types of step edges.

where multiple TL occurs, the chemical selectivity between these TL has already been used in terms of selective etching. Another way to recover a single TL is to develop new masking techniques based on the same selectivity. Therefore, we have developed a *general procedure* that finally opens a door to the local identification of the various TLs of layered materials and hence to the controlled modification of UCs, tailoring their properties to an extent never accessible in bulk compounds.

The authors thank H.-J. Güntherodt, E. Meyer, J. G. Bednorz, C. Rossel, R. Allenspach, and H. Siegenthaler for useful discussions, and the Swiss National Science Foundation (NFP36) as well as the Swiss Priority Project "Minast" for financial support.

[1] J. G. Bednorz and K. A. Müller, Z. Phys. B **64**, 189 (1986).
[2] K. Chahara, T. Ohono, M. Kasai, and Y. Kozono, Appl. Phys. Lett. **63**, 1990 (1993); R. von Helmholt, J. Wecker, B. Holzapfel, L. Schultz, and K. Samwer, Phys. Rev. Lett. **72**, 2331 (1993).
[3] C. A.-Paz de Araujo, J. D. Cuchiaro, L. D. McMillan, M. C. Scott, and J. F. Scott, Nature (London) **374**, 627 (1995).
[4] For a review, see for instance, J. N. Eckstein and I. Bozovic, Annu. Rev. Mater. Sci. **25**, 679 (1995).
[5] T. Terashima, K. Shimura, Y. Bando, Y. Matsuda, A. Fujiyama, and S. Komiyama, Phys. Rev. Lett. **67**, 1362 (1991).
[6] Q. Li, C. Kwon, X. X. Xi, S. Bhattacharya, A. Walkenhorst, T. Venkatesan, S. J. Hagen, W. Jiang, and R. L. Greene, Phys. Rev. Lett. **69**, 2713 (1992).
[7] J.-M. Triscone, Ø. Fischer, O. Brunner, L. Antognazza, A. D. Kent, and M. G. Karkut, Phys. Rev. Lett. **64**, 5176 (1990).
[8] I. N. Chan, D. C. Vier, O. Nakamura, J. Hasen, J. Guimpel, S. Schultz, and I. K. Schuller, Phys. Lett. A **175**, 241 (1993).
[9] N. Chandrasekhar, V. S. Achutharaman, V. Agrawal, and A. M. Goldman, Phys. Rev. B **46**, 8565 (1992).
[10] Similar stacks were suggested in V. C. Matijasevic, B. Ilge, B. Stäuble-Pümpin, G. Rietveld, F. Tuinstra, and J. E. Mooij, Phys. Rev. Lett. **76**, 4765 (1996); T. Haage, Q. D. Jiang, M. Cardona, H.-U. Habermeier, and J. Zegenhagen, Appl. Phys. Lett. **68**, 2427 (1996).
[11] J. G. Wen, C. Traeholt, and H. W. Zandbergen, Physica C **205**, 354 (1993).
[12] K. Shimura, Y. Daitoh, Y. Yano, T. Terashima, Y. Bando, Y. Matsuda, and S. Komiyama, Physica C **228**, 91 (1994).
[13] S. J. Pennycook, M. F. Chrisholm, D. E. Jesson, D. P. Norton, D. H. Lowndes, R. Feenstra, H. R. Kerchner, and J. O. Thomson, Phys. Rev. Lett. **67**, 765 (1991).
[14] H. L. Edwards, J. T. Markert, and A. L. de Lozanne, Phys. Rev. Lett. **69**, 2967 (1992).
[15] S. Tanaka, T. Nakamura, M. Iijama, N. Yoshida, S. Takano, F. Shoji, and K. Oura, Appl. Phys. Lett. **59**, 3637 (1991).
[16] J.-P. Locquet and E. Mächler, Mater. Res. Bull. **19**, 39 (1994).
[17] T. Hikita, T. Hanada, M. Kudo, and M. Kawai, J. Vac. Sci. Technol. A **11**, 2649 (1993).
[18] M. Yoshimoto, T. Maeda, K. Shimozono, H. Koinuma, M. Shinohara, O. Ishiyama, and F. Ohtani, Appl. Phys. Lett. **65**, 3197 (1994).
[19] T. Nakamura, H. Inada, and M. Iiyama, Jpn. J. Appl. Phys., Part 1 **36**, 90 (1997).
[20] M. Kawasaki, K. Takahashi, T. Maeda, R. Tsuchiya, M. Shinohara, O. Ishiyama, T. Yonezawa, M. Yoshimoto, and H. Koinuma, Science **266**, 1540 (1994) reported that etching in buffered NH_4–HF preferentially removes SrO, although this process is not 100% selective as reported by P. A. Bertrand and P. D. Fleischauer, Thin Solid Films **103**, 167 (1983); K. S. Young and Y. W. Lam, Thin Solid Films **109**, 169 (1983).
[21] ESCETE, Single Crystal Technology, B. V., NL–7547 RD Enschede, The Netherlands. The etching process used is similar to that in Ref. 20.
[22] The SFM analysis was performed with a Nanoscope III system from Digital Instruments (Santa Barbara, CA) in contact, friction, and tapping mode. The scan unit was placed in an argon-filled bag, which was attached to the annealing chamber and sealed against the ambient. Cantilevers were changed *in situ*, and their geometry was analyzed later by means of scanning electron microscopy to calculate the cantilever spring constants. For details see E. Meyer, R. Lüthi, L. Howald, M. Bammerlin, M. Guggisberg, and H.-J. Güntherodt, in *Micro/Nanotribology and Its Applications*, NATO ASI Series E: Appl. Sci., edited by B. Bhusan (Kluwer, Dordrecht, 1997), Vol. 330, pp. 193–215. Contact and tapping modes revealed similar topography images, but only contact-mode results are presented here. For this mode we used Si sensors (Nanosensors, Aidlingen, Germany) with a spring constant of 0.26 N/m and a torsional spring constant of 106 N/m.
[23] S. M. Paik, S. Kim, and I. K. Schuller, Phys. Rev. B **44**, 3272 (1991).
[24] B. Stäuble-Pümpin, B. Ilge, V. C. Matijasevic, P. M. L. O. Scholte, A. J. Steinfort, and F. Tuinstra, Surf. Sci. **369**, 313 (1996); R. Sum, H. P. Lang, and H.-J. Güntherodt, Physica C **242**, 174 (1995).
[25] Friction contrast was observed between a substrate and a deposit, see for instance L. Howald, E. Meyer, R. Lüthi, H. Haefke, R. Overney, H. Rudin, and H.-J. Güntherodt, J. Vac. Sci. Technol. B **12**, 2227 (1994); J. Tamayo, R. García, T. Utzmeier, and F. Briones, Phys. Rev. B **55**, R13436 (1997); B. Bhushan, J. N. Israelachvili, and U. Landman, Nature (London) **359**, 133 (1995).
[26] V. E. Henrich, G. Dresselhaus, and H. J. Ziegler, Phys. Rev. B **17**, 4908 (1978); B. Cord and R. Courths, Surf. Sci. **162**, 34 (1985); T. Matsumoto, H. Tanaka, T. Kawai, and S. Kawai, Surf. Sci. Lett. **278**, L153 (1992).
[27] Q. D. Jiang and J. Zegenhagen, Surf. Sci. **367**, L42 (1996); H. Bando, Y. Aiura, Y. Haruyama, T. Shimizu, and Y. Nishihara, J. Vac. Sci. Technol. B **13**, 1150 (1995).
[28] T. Nishihara, O. Ishiyama, S. Hayashi, M. Shinohara, M. Yoshimoto, T. Ohnishi, and H. Koinuma, in *Proceedings of MRS Spring Meeting, Symposium on Epitaxial Oxide Thin Films,* Vol. 474 (Materials Research Society, Warrendale, PA, 1997), contrary to Ref. 26, these authors also suggest an increased Ti desorption, possibly due to ignoring ordered oxygen vacancies in their data deconvolution.
[29] S. Suzuki, H. Ohsaki, and E. Ando, Jpn. J. Appl. Phys., Part 1 **35**, 1862 (1996).
[30] J. Jorgensen, M. A. Beno, D. G. Hinks, L. Soderholm, K. J. Volin, R. L. Hitterman, J. D. Grace, I. K. Schuller, C. U. Segre, and K. Zhang, Phys. Rev. B **36**, 3608 (1987).

PROCEEDINGS OF SPIE REPRINT

SPIE—The International Society for Optical Engineering

Reprinted from

Superconducting and Related Oxides: Physics and Nanoengineering III

20–24 July 1998
San Diego, California

Volume 3481

Critical temperature enhancement by means of substrate-induced pressure

J. Perret[a,b], J. Fompeyrine[b], J. W. Seo[a,b], E. Mächler[b],
Ø. Fischer[c], P. Martinoli[a] and J.-P. Locquet[b]

[a]Institut de Physique, Université de Neuchâtel, CH-2000 Neuchâtel, Switzerland

[b]IBM Research Division, Zurich Research Laboratory, CH-8803 Rüschlikon, Switzerland

[c]DPMC, Université de Genève, CH-1211 Genève, Switzerland

ABSTRACT

In the field of high-temperature superconductivity there has been no increase in the critical temperature T_c of bulk compounds since 1993. However, an analysis of the uniaxial strain or pressure derivatives of T_c in the cuprate superconductors allows us to predict that under a compressive epitaxial strain, a large increase of T_c should be possible. We demonstrate the experimental feasibility of this approach for $La_{2-x}Sr_xCuO_{4\pm\delta}$ ("214") thin films deposited on (001)-oriented $SrLaAlO_4$ substrates for different Sr content ($0.045 \leq x \leq 0.11$). Under epitaxial strain, a large jump of the critical temperature T_c is observed, as well as a drastic change in the resistive behavior from insulating to metallic at low temperatures.

Keywords: Cuprate, Superconductivity, Oxide, Thin Films, Epitaxial Strain

1. INTRODUCTION

The pressure dependence of the superconducting transition temperature T_c is an important quantity to optimize a material as well as to investigate the nature of the superconducting state. A strong dependence indicates that the material is able to reach higher values of T_c at ambient pressure, for example by doping in order to change the electronic structure or to invoke "chemical" pressure. Pressure is also a "clean" and controlled means to change the lattice parameters of the system and check theoretical predictions.

Most of the experiments as well as theoretical calculations are based on hydrostatic or quasihydrostatic pressure. The pressure (P) and strain ($\epsilon = [d_{\text{bulk}} - d_{\text{strained}}]/d_{\text{bulk}}$, where d is a lattice parameter) dependence of T_c for a tetragonal unit cell contains an in-plane (ab) and an out-of-plane (c) term, and can be written

$$\begin{aligned} T_c &= T_c(0) + 2\frac{\delta T_c}{\delta P_{ab}}P + \frac{\delta T_c}{\delta P_c}P \\ &= T_c(0) + 2\frac{\delta T_c}{\delta \epsilon_{ab}}\epsilon_{ab} + \frac{\delta T_c}{\delta \epsilon_c}\epsilon_c \,. \end{aligned} \tag{1}$$

For most systems,[1] the in-plane and out-of-plane T_c derivatives have opposite signs, leading to a partial cancellation of the hydrostatic pressure effects.[2] For these reasons, and because of the large intrinsic anisotropy of the cuprate superconductors, uniaxial deformations are required in order to isolate the different contributions responsible for any change of the superconducting properties. However, under epitaxial growth conditions, ϵ_{ab} and ϵ_c normally have opposite signs, and these two terms add up to increase (compressive, $\epsilon_{ab} > 0$) or decrease (tensile, $\epsilon_{ab} < 0$) T_c.

Several groups have succeeded in inducing a high-pressure state in thin films by using epitaxial strain,[3,4] but only moderate increases of T_c have been reported.[5,6] In the case of epitaxially grown c-axis thin films we deal with a permanent biaxial pressure applied in the ab-plane by the substrate on the film. The magnitude of the effect depends on the ability to keep the strain inside the growing structure as long as possible. Hence, the optimal thickness of the film is a compromise between avoiding the nucleation of misfit dislocations and minimizing the T_c reduction observed

Other author information: (Send correspondence to J. Perret.)
J. Perret: E-mail: joel.perret@iph.unine.ch
J.-P. Locquet: E-mail: loc@zurich.ibm.com

In Superconducting and Releted Oxides: Physics and Nenoengineering III,
D. Pavuna and I. Bozovic, editors, Proceedings of SPIE Volume 3481 (July 1998)
[0277-786X/98/$10.00]

for ultrathin films.[7,8] Indeed, dislocations appear when a critical thickness h_c has been exceeded;[9] h_c decreases with increasing mismatch, suggesting that a large strain requires very thin films. The aim of this report is to emphasize the relations between these two fundamental aspects (induced pressure and synthesis) of thin-film growth.

Among the high-T_c cuprates, $La_{2-x}Sr_xCuO_{4\pm\delta}$ has the simplest crystallographic structure. This compound can be grown in a wide range of concentration of mobile charge carriers by varying the Sr content. For the bulk-related compound the lower limit of concentration is about $x = 0.06$, whereas in the overdoped region superconductivity is suppressed beyond $x = 0.25$. The value of T_c reaches a maximum of 37 K for $x = 0.15 - 0.16$. Another way to improve the transport properties of the strontium doped "214" compound is to increase its oxidation level by electrochemistry.[10,11] The critical temperature reached in this way does not exceed 40 K for the entire oxygen doping range ($0 \leq \delta \leq 0.135$). Both strontium and oxygen content can significantly change the lattice parameters and T_c, masking the exact origin of an enhancement of the superconducting properties.

The choice of a suitable substrate is crucial for the quality of the deposited superconducting film. In-plane lattice parameters, thermal expansion coefficients, and dielectric and interdiffusion constants are some of the parameters which we have to take into account. The most common substrate used for the growth of cuprate superconductors is $SrTiO_3$ (STO). The mismatch between the lattice parameters of the latter and of the "214" is about +3.1%, inducing a expansion of the *a*- and *b*-axis of the film (tensile strain). Previous studies have shown that critical superconducting temperatures of thin films deposited on STO are strongly depressed compared to the bulk ones.[12–15] We observe a T_c above 30 K only for thicknesses beyond 500 nm, where the mismatch between the film and the substrate becomes partially accommodated by the misfit dislocation pattern. In the case of $SrLaAlO_4$ (SLAO) substrates, the deposited thin film will be slightly compressed due to a small negative mismatch (−0.60%). Other groups[5,16,17] have succeeded in growing high-quality "214" thin films on SLAO substrates. Values of T_c reached were as high and even higher than those obtained for the bulk compounds.

2. EXPERIMENTAL DETAILS

The samples studied in this report were thin (12 unit cells) films of $La_{2-x}Sr_xCuO_{4\pm\delta}$ deposited simultaneously on high-quality, (001)-oriented SLAO and (100)-oriented STO substrates. We focused our study on the highly underdoped region ($0.045 \leq x \leq 0.11$) where the strain is expected to be maximum. The sample fabrication details have been reported elsewhere.[18] In brief, thin films were grown in a molecular beam epitaxy (MBE) system equipped with four effusion cells (one for strontium), two electron beam guns (for copper and lanthanum), two quartz monitors, a reflection of high-energy electron diffraction (RHEED) system, an efficient RF plasma source of atomic oxygen, and three quadrupole mass-spectrometers. The latter allowed us to control the beam flux and were calibrated using the quartz monitors. The method used to grow epitaxial thin films consists of a block-by-block deposition.[19] The sequential deposition starts with $2-x$ monolayers of La-O, x monolayers of Sr-O, and one monolayer of Cu-O followed by a 10-sec waiting step under a continuous flow of atomic oxygen. We have shown previously that high-quality films can be grown with this method. The base pressure of the system is of the order of 10^{-9} Torr, whereas during the deposition, the partial O_2 pressure is about 5×10^{-6} Torr. The substrate temperature measured with a pyrometer operated in the infrared (8–14 μm) was 770 °C, and the deposition rate was approximately 0.5 unit cells per minute. The cool down is rather fast, the heater power being switched off, but the plasma source oxidizes the sample until it reaches room temperature.

3. RESULTS AND DISCUSSION

During the deposition, long vertical streak patterns showed by the RHEED indicate a nearly two-dimensional growth. There is also an extra modulation visible between the streaks (Fig. 1). The accuracy with which we determined the effective Sr content is not better than 10%. The Sr doping level is estimated from Hall measurements performed at 100 K on thin films deposited on STO.[18] The values of the inverse Hall coefficient given in Ref. 15, as well as the two end points of the phase diagram (T_c,x) on STO, were used to calibrate our strontium content.

Usually, the oxidation level is a confusing issue because it is difficult to measure it accurately. In our case the parent compound $La_2CuO_{4\pm\delta}$ may be doped with oxygen in a small range by different techniques, allowing samples to reach critical temperatures as high as 44 K.[20–22] However, strontium incorporation in this material depresses its transition to 40 K. The fact that underdoped ($x < 0.045$) $La_{2-x}Sr_xCuO_{4\pm\delta}$ thin films deposited on STO and on SLAO exhibit semiconducting-like rather than superconducting behavior at low temperatures proves that the oxygen excess is negligible in these samples. Moreover, high-temperature post-annealing stages under a continuous flow of molecular oxygen do not improve the transport properties of our films significantly.

Figure 1. Typical RHEED image subsequent to the deposition.

3.1. Structural properties

The x-ray diffraction experiments confirm the c-axis-oriented growth for all our films deposited on SLAO and STO (Fig. 2). Finite-size effect oscillations were observed at low angle and around (00ℓ) peaks ($\ell = 2, 4, 6$), allowing a good estimate of effective thin-film thicknesses. Such oscillations are not present in films containing large fluctuations of thickness. From usual $\theta - 2\theta$ scans and measurements taken around the (107), (109) and (1011) reflections, the lattice parameters c = 13.31 ± 0.01 Å and a = 3.76 ± 0.02 Å were determined for the film deposited on SLAO (bulk compound[23]: 13.212 and 3.784 Å), leading to $\epsilon_{ab} = 0.63\%$, $\epsilon_c = -0.76\%$. For the film grown on STO, similar measurements yield $\epsilon_{ab} = -0.54\%$, $\epsilon_c = 0.35\%$. The full width at half maximum (FWHM) of the rocking curves around the (004) peak are about 0.07° degrees on SLAO, close to that of the substrates (0.06°), whereas on STO the smallest value obtained is about 0.12°. Off-axis measurements around the (1011) peak taken on both films emphasize a large in-plane coherence obtained on SLAO by the appearance of finite-size oscillations (Fig. 3). The latter are not visible on STO, indicating a smaller in-plane coherence. The transmission electron microscopy (TEM) analysis

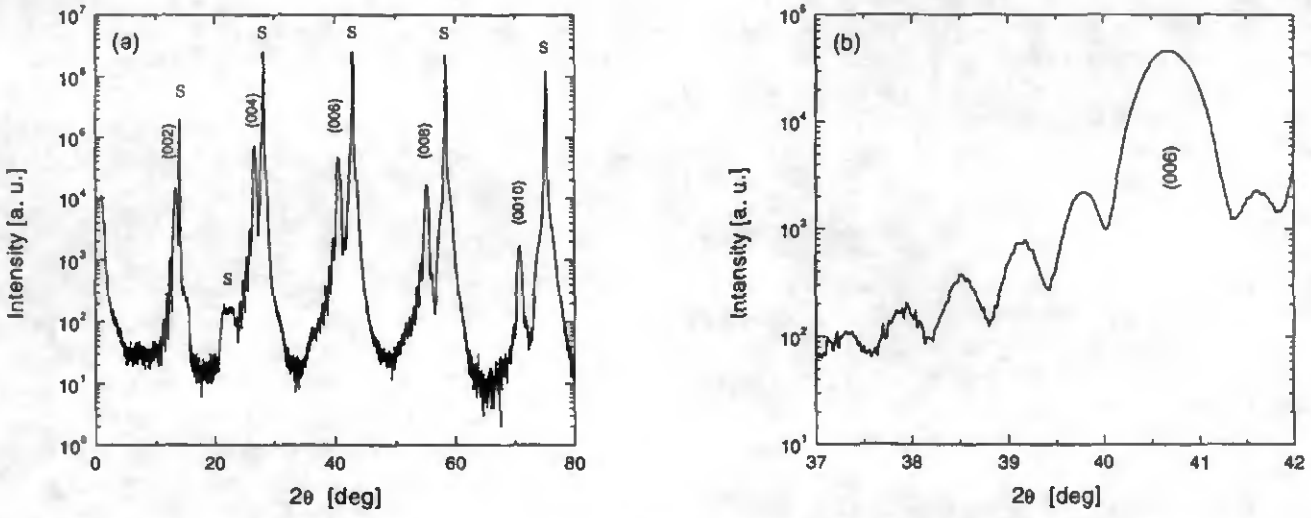

Figure 2. (a) X-ray diffraction pattern of a 12 unit-cell-thick $La_{2-x}Sr_xCuO_{4\pm\delta}$ film on SLAO. Besides the substrate peaks indicated by S, only the "214" (00ℓ) reflections with their finite-size effect oscillations are observed. (b) Zoom of the (006) reflection.

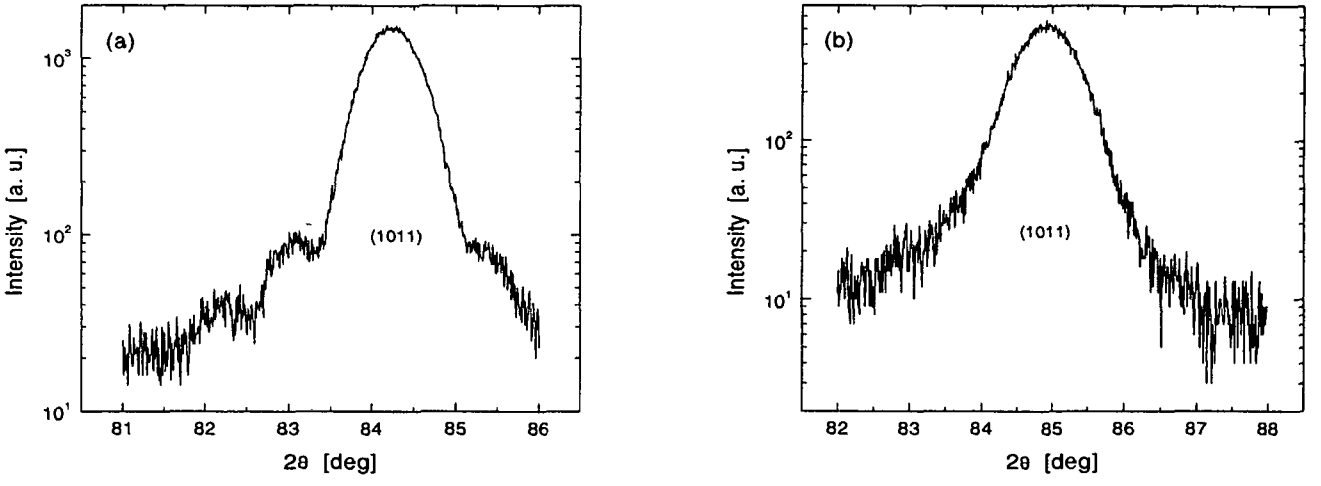

Figure 3. Off-axis $\theta - 2\theta$ diffraction spectrum around the (1011) reflection for the film (a) on SLAO and (b) on STO.

of these films[24] confirms the higher crystallinity of the film on SLAO.

3.2. Transport properties

The behavior of cuprate superconductors above their critical temperature remains mysterious. A better understanding of the normal-state properties could help us toward a complete theory of these materials. Here we focus our analysis on the behavior of thin films with a strontium content of $x = 0.10$, which seems to be the optimal doping level (highest T_c) under the compressive strain achievable on SLAO.

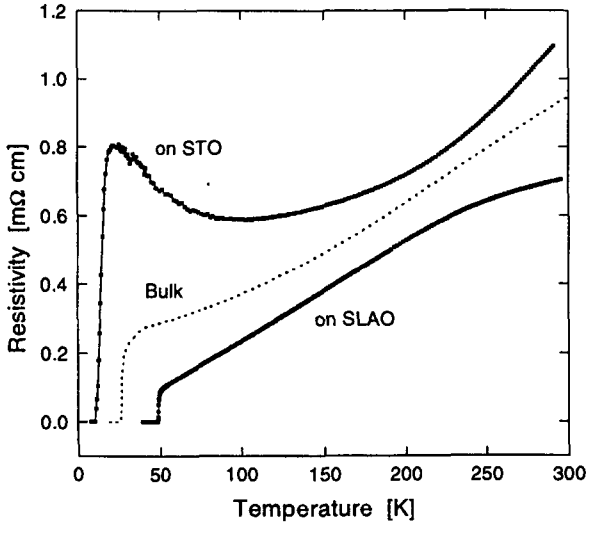

Figure 4. Resistivity versus temperature for two films grown simultaneously on STO and SLAO and for a bulk single crystal[25] (dotted line). The strontium content is the same for the three samples ($x = 0.10$).

The values of ϵ determined in the previous section as well as the strain derivatives $\delta T_c/\delta\epsilon$ for the "214" compound[26,27] suggest an important increase of T_c. Resistivity measurements (Fig. 4) performed on two underdoped ($x = 0.10$) samples grown simultaneously on different substrates show that the film grown under compressive strain on SLAO has a $T_c(R = 0)$ of 49.1 K, whereas the film grown under tensile strain on STO has a $T_c(R = 0)$ of only 10 K. Compared to the T_c of 25 K for the bulk compound,[25] these values show how large the epitaxial strain effects can be. Such large variations of the critical temperature have not been achieved for the bulk "214", not even under the highest hydrostatic or uniaxial pressure used to date. Only an in-plane bi-axial pressure could lead to such a change in T_c. The width of the transition on SLAO is extremely sharp $\delta T_c = 0.7$ K, whereas on STO the value of $\delta T_c = 4$ K might be related to the presence of planar defects.[24]

Another significant change occurs in the normal-state resistivity of these films. The resistivity $\rho(T)$ of the film grown under tensile strain (on STO) exhibits a significant upturn before the onset of superconductivity. This behavior is expected for highly underdoped bulk "214" ($x < 0.08$).[25] Under compressive strain (on SLAO) the resistivity shows a linear and metallic behavior, which is usually observed for optimally doped compound ($x = 0.16$). The small change in slope at about 260 K could be interpreted as an indication of the development of a pseudogap in the excitation spectrum. For the bulk compound, however, such a change of slope starts at higher temperatures.[28] Hence, in addition to the drastic increase of T_c, epitaxial strain also modifies the normal-state properties of "214".

The superconductor–insulator transition in "214" thin films under compressive strain occurs at a lower strontium concentration ($x \approx 0.045$) compared to that of the bulk ($x = 0.06$). Moreover, this transition seems to be very sharp; the film goes abruptly from an insulating to a superconducting state with a T_c of 37 K as shown in Fig. 5.

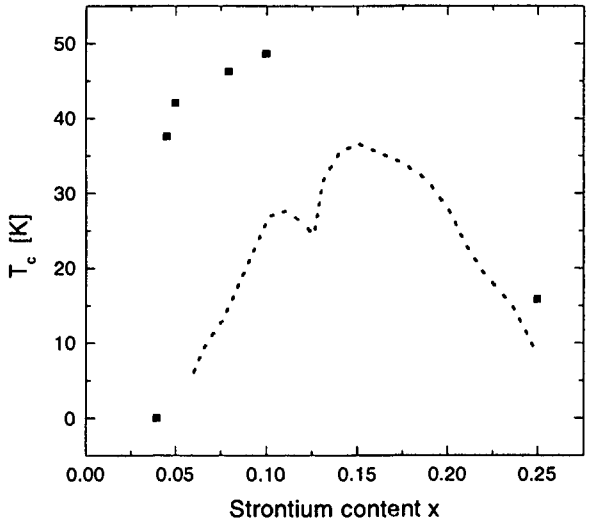

Figure 5. $T_c(R = 0)$ dependence on strontium content x for "214" thin films grown under epitaxial strain. The dotted line corresponds to "214" bulk data.[29]

4. CONCLUSIONS

The results obtained on $La_{2-x}Sr_xCuO_{4\pm\delta}$ thin films grown under epitaxial strain give rise to some comments. It is interesting to emphasize that the highest T_c on SLAO appears to be reached for $x = 0.10$. Invoking an increase of the carrier density due to a reduction of the in-plane surface under compressive strain is not sufficient to explain such a variation. Indeed, a change in the carrier density of $\pm 10\%$ would result in a total T_c variation of 7 K in the bulk phase diagram, and not $\simeq$40 K as we observed. Moreover, previous Hall coefficient measurements on bulk "214" showed a very small pressure dependence, ruling out a large pressure-induced carrier density change.[30]

Measurements of c-axis resistivities as a function of pressure indicates clearly that ρ_c decreases as the c-axis parameter in bulk "214" decreases.[31] In spite of the difficulty of identifying and quantifying which lattice deformation (in-plane or out-of-plane) is responsible for the changes in the transport properties, the data for this compound reveal that T_c increases with increasing distance between consecutive CuO_2 planes, which contradicts certain theoretical predictions concerning interlayer coupling.[32] Further work should help us to gain a better understanding of the fundamental mechanisms that lead to high-temperature superconductivity.

ACKNOWLEDGMENTS

We thank Y. Jaccard, E. J. Williams, A. Rüfenacht, D. Ariosa, and M. Calame for helpful discussions. This work was supported by the Swiss National Science Foundation.

REFERENCES

1. J.-P. Locquet, J. Perret, J. Fompeyrine, E. Mächler, J. W. Seo, and G. Van Tendeloo, "Doubling the critical temperature of $La_{1.9}Sr_{0.1}CuO_4$ using epitaxial strain," *Nature*, 1998. in press.
2. U. Welp, M. Grimsditch, S. Fleshler, W. Nessler, J. Downey, and G. W. Crabtree, "Effect of uniaxial stress on the superconducting transition in $YBa_2Cu_3O_7$," *Phys. Rev. Lett.* **69**, pp. 2130–2133, 1992.
3. S. L. Bud'ko, J. Guimpel, O. Nakamura, M. B. Maple, and I. K. Schuller, "Uniaxial pressure dependence of the superconducting critical temperature in $RBa_2Cu_3O_{7-\delta}$ high-T_c oxides," *Phys. Rev. B* **46**, pp. 1257–1260, 1992.
4. G. L. Belenky, S. M. Green, A. Roytburd, C. J. Lobb, S. J. Hagen, R. L. Green, M. G. Forrester, and J. Talvacchio, "Effect of stress along the *ab* plane on the J_c and T_c of $YBa_2Cu_3O_7$ thin films," *Phys. Rev. B* **44**, pp. 10117–10120, 1991.
5. H. Sato and M. Naito, "Increase in the superconducting transition temperature by anisotropic strain effect in (001) $La_{1.85}Sr_{0.15}CuO_4$ thin films on $LaSrAlO_4$ substrates," *Physica C* **274**, pp. 221–226, 1997.
6. J.-P. Locquet and E. J. Williams, "Epitaxially induced defects in Sr- and O-doped La_2CuO_4 thin films grown by MBE: implications for transport properties," *Acta Polonica A* **92**, pp. 69–84, 1997.
7. J.-M. Triscone, Ø. Fischer, O. Brunner, L. Antognazza, A. D. Kent, and M. G. Karkut, "$YBa_2Cu_3O_7/PrBa_2Cu_3O_7$ superlattices: Properties of ultrathin superconducting layers separated by insulating layers," *Phys. Rev. Lett.* **64**, pp. 804–807, 1990.
8. T. Terashima, K. Shimura, Y. Bando, Y. Matsuda, A. Fujiyama, and S. Komiyama, "Superconductivity of one-unit-cell thick $YBa_2Cu_3O_7$ thin film," *Phys. Rev. Lett.* **67**, pp. 1362–1365, 1991.
9. J. W. Matthews and A. E. Blakeslee, "Defects in epitaxial multilayers," *J. Cryst. Growth* **27**, pp. 118–125, 1994.
10. F. C. Chou, J. H. Cho, and D. C. Johnston, "Synthesis, characterization, and superconducting and magnetic properties of electrochemically oxidized $La_2CuO_{4+\delta}$ and $La_{2-x}Sr_xCuO_{4+\delta}$ ($0.01 \leq x \leq 0.33, 0.01 \leq \delta \leq 0.36$)," *Physica C* **197**, pp. 303–314, 1992.
11. C. Rial, E. Morán, M. A. Alario-Franco, U. Amador, and N. H. Andersen, "Structural and superconducting properties of $La_{2-x}Sr_xCuO_{4+y}$ ($0 < x < 0.15$) prepared by room temperature chemical oxidation," *Physica C* **254**, pp. 233–248, 1995.
12. M. Suzuki, "Hall coefficients and optical properties of $La_{2-x}Sr_xCuO_4$ single-crystal thin films," *Phys. Rev. B* **39**, pp. 2312–2321, 1989.
13. M. Suzuki and M. Hikita, "Resistive transition, magnetoresistance, and anisotropy in $La_{2-x}Sr_xCuO_4$ single-crystal thin films," *Phys. Rev. B* **44**, pp. 249–261, 1991.
14. H. L. Kao, J. Kwo, R. M. Fleming, M. Hong, and J. P. Mannearts, "*In situ* growth and properties of single-crystalline-like $La_{2-x}Sr_xCuO_4$ epitaxial films by off-axis sputtering," *Appl. Phys. Lett.* **59**, pp. 2748–2750, 1991.
15. J.-P. Locquet, Y. Jaccard, A. Cretton, E. J. Williams, F. Arrouy, E. Mächler, T. Schneider, Ø. Fischer, and P. Martinoli, "Variation of the in-plane penetration depth λ_{ab} as a function of doping in $La_{2-x}Sr_xCuO_{4\pm\delta}$ thin films on $SrTiO_3$: Implication for the overdoped state," *Phys. Rev. B* **54**, pp. 7481–7488, 1996.
16. I. E. Trofimov, L. A. Johnson, K. V. Ramanujachary, S. Guha, M. G. Harrison, M. Greenblatt, M. Z. Cieplak, and P. Lindenfeld, "Growth and properties of $La_{2-x}Sr_xCuO_4$ films," *Appl. Phys. Lett.* **65**, pp. 2481–2483, 1994.
17. M. Z. Cieplak, M. Berkowski, S. Guha, E. Cheng, A. S. Vagelos, D. J. Rabinowitz, B. Wu, I. E. Trofimov, and P. Lindenfeld, "Thickness dependence of $La_{2-x}Sr_xCuO_4$ films," *Appl. Phys. Lett.* **65**, pp. 3383–3385, 1994.

18. Y. Jaccard, A. Cretton, E. J. Williams, J.-P. Locquet, E. Mächler, C. Gerber, T. Schneider, Ø. Fischer, and P. Martinoli, "Characterization of MBE-grown ultrathin films in the $La_{2-x}Sr_xCuO_{4\pm\delta}$ system," in *Oxide Superconductor Physics and Nano-Engineering, Proc. SPIE* **2158**, pp. 200–210, 1994.
19. J.-P. Locquet, A. Catana, E. Mächler, C. Gerber, and J. G. Bednorz, "Block-by-block deposition: A new growth method for complex oxide thin films," *Appl. Phys. Lett.* **64**, pp. 372–374, 1994.
20. A. Wattiaux, J. C. Park, J. C. Grenier, and M. Pouchard, "Une nouvelle voie d'accès aux oxydes supraconducteurs : l'oxydation électrochimique de La_2CuO_4," *C.R. Acad. Sci. Paris* **310(II)**, pp. 1047-1052, 1990.
21. J.-P. Locquet, C. Gerber, A. Cretton, Y. Jaccard, E. J. Williams, and E. Mächler, "Electrochemical oxidation of La_2CuO_4 thin films grown by molecular beam epitaxy," *Appl. Phys. A* **57**, pp. 211–215, 1993.
22. F. Arrouy, J.-P. Locquet, E. J. Williams, E. Mächler, R. Berger, C. Gerber, C. Monroux, J.-C. Grenier, and A. Wattiaux, "Growth, microstructure, and electrochemical oxidation of MBE-grown *c*-axis La_2CuO_4 thin films," *Phys. Rev. B* **54**, pp. 7512–7520, 1996.
23. P. G. Radaelli, D. G. Hinks, A. W. Mitchell, B. A. Hunter, J. L. Wagner, B. Dabrowski, K. G. Vandervoort, H. K. Viswanathan, and J. D. Jorgensen, "Structural and superconducting properties of $La_{2-x}Sr_xCuO_4$ as a function of Sr content," *Phys. Rev. B* **53**, pp. 4163–4175, 1994.
24. J. W. Seo, J. Perret, J. Fompeyrine, G. Van Tendeloo, and J.-P. Locquet, "Microstructural investigation of $La_{1.9}Sr_{0.1}CuO_4$ thin films grown by MBE," *these proceedings.*
25. T. Kimura, S. Miyasaka, H. Takagi, K. Tamasaku, H. Eisaki, S. Uchida, K. Kitazawa, M. Hiroi, M. Sera, and N. Kobayashi, "In-plane and out-of-plane magnetoresistance in $La_{2-x}Sr_xCuO_4$ single crystals," *Phys. Rev. B* **53**, pp. 8733–8742, 1996.
26. M. Nohara, T. Suzuki, Y. Maeno, T. Fujita, I. Tanaka, and H. Kojima, "Unconventional lattice stiffening in superconducting $La_{2-x}Sr_xCuO_4$ single crystals," *Phys. Rev. B* **52**, pp. 570–580, 1995.
27. F. Gugenberger, C. Meingast, G. Roth, K. Grube, V. Breit, T. Weber, H. Wühl, S. Uchida, and Y. Nakamura, "Uniaxial pressure dependence of T_c from high-resolution dilatometry of untwinned $La_{2-x}Sr_xCuO_4$ single crystals," *Phys. Rev. B* **49**, pp. 13137–13142, 1994.
28. B. Batlogg, H. Y. Hwang, H., R. J. Cava, H. L. Kao, and J. Kwo, "Normal state phase diagram of $(La,Sr)_2CuO_4$ from charge and spin dynamics," *Physica C* **235-240**, pp. 130–133, 1994.
29. H. Takagi, T. Ido, S. Ishibishi, M. Uota, S. Uchida, and Y. Tokura, "Superconductor-to-nonsuperconductor transition in $(La_{1-x}Sr_x)_2CuO_4$," *Phys. Rev. B* **40**, pp. 2254–2261, 1989.
30. N. Tanahashi, Y. Iye, T. Tamegai, C. Murayama, N. Môri, S. Yomo, N. Okazaki, and K. Kitazawa, "The strontium content dependence of pressure effect in $(La_{1-x}Sr_x)_2CuO_4$," *Jpn. J. Appl. Phys.* **28**, pp. L762–L765, 1989.
31. F. Nakamura, M. Kodama, S. Sakita, Y. Maeno, T. Fujita, H. Takahashi, and N. Môri, "Pressure dependence of out-of-plane conduction in $La_{2-x}Sr_xCuO_4$," *Phys. Rev. B* **54**, pp. 10061–10064, 1996.
32. P. W. Anderson, *The Theory of Superconductivity in the High-T_c Cuprate Superconductors*, Princeton Univ. Press, Princeton, NJ, 1997.

PROCEEDINGS OF SPIE REPRINT

SPIE—The International Society for Optical Engineering

Reprinted from

Superconducting and Related Oxides: Physics and Nanoengineering III

20–24 July 1998
San Diego, California

Volume 3481

Microstructural investigation of $La_{1.9}Sr_{0.1}CuO_4$ thin films grown by MBE

J. W. Seo[a,b], J. Perret[a,b], J. Fompeyrine[b], G. Van Tendeloo [c] and J.-P. Locquet[b]

[a]Institut de Physique, Université de Neuchâtel, CH-2000 Neuchâtel, Switzerland

[b]IBM Research Division, Zurich Research Laboratory, CH-8803 Rüschlikon, Switzerland

[c]EMAT, RUCA University of Antwerp, B-2020 Antwerpen, Belgium

ABSTRACT

The microstructure of $La_{1.9}Sr_{0.1}CuO_4$ thin films grown by molecular beam epitaxy on $SrLaAlO_4$ and $SrTiO_3$ is investigated by transmission electron microscopy. Using $SrLaAlO_4$ as substrate material, compressive strain is induced, which leads to a drastic increase of T_c. In contrast, $SrTiO_3$ yields a tensile strain and a decrease of T_c. The film on $SrLaAlO_4$ has a low defect density. Only misfit dislocations with an average spacing of 200 nm are found, which are more or less irregularly distributed. For $SrTiO_3$, a periodic array of misfit dislocations is present with an average distance of 16 nm. At the interface, as derived from the comparison with simulated images, $(LaSr)_2CuAlO_{6-x}$ and $(LaSr)TiO_{3-x}$ are formed on $SrLaAlO_4$ and $SrTiO_3$, respectively. These intermediate layers are found to increase the corresponding compressive and tensile strain further. The lattice deformation is determined based on lattice-image analysis. Here, the distance of CuO_2 planes can be measured locally. It turns out that applying a compressive or tensile strain increases or decreases the distance between CuO_2 planes. Accordingly, direct evidence is presented that a decoupling of CuO_2 planes leads to an increase of T_c, which is in contradiction to recent theoretical predictions.

Keywords: Superconductivity, Cuprate, Thin Films, Epitaxial Strain, Microstructure, TEM

1. INTRODUCTION

The critical temperature T_c of a high-temperature superconductor can be increased by applying hydrostatic pressure.[1] Unfortunately, this state is not stable when the pressure is relieved. The comparable pressure effect can also be obtained and stabilized by applying an epitaxial strain,[2,3] i.e., by using the lattice mismatch between the film and its substrate in an epitaxial film growth. So far, only moderate increases of T_c have been reported.[4,5] To increase T_c significantly, it has been shown that the amount and, in particular, the sign of the induced strain ϵ are essential.[5,6] The term ϵ is defined by the relative lattice deformation $\epsilon = (d_{Bulk} - d_{Film})/d_{Bulk}$ (where d is a lattice parameter) and contains two terms, $\epsilon = f - \delta$, where f is the lattice mismatch between the film and substrate and δ is the plastic strain associated with the incorporation of dislocations. It is known that the introduction of dislocations starts when the film thickness exceeds the critical value h_c at which the strain relaxation is initiated.[7-9] Consequently, the highest amount of elastic strain can only be induced in a very thin film with a thickness of less than h_c.

Indeed, by optimizing these parameters,[5,10] we succeeded for the first time to increase T_c drastically by applying compressive epitaxial strain.[6] The deposition of $La_{2-x}Sr_xCuO_4$ ("214") on $SrLaAlO_4$ (SLAO) yields a doubling of T_c (49 K) compared to the bulk material (25 K) with the same composition.[11] In contrast, the equivalent "214" thin film grown simultaneously on $SrTiO_3$ (STO), which yields a tensile strain,[5,10] showed a decrease of T_c (10 K).[6] The tensile strain might be the explanation for the low T_c values measured up to now for all "214" thin films grown on STO.[5,12]

In order to correlate the drastic change of T_c with the actual amount and sign of the epitaxial strain, it is essential to study the microstructural property of these films in detail. In recent years, it has been shown that lattice defects in high-T_c superconductors can have an important effect on the physical properties of the materials.[5,13-15] In particular, for stress-induced films the amount of the strain is directly related to the presence of defects and consequently to T_c. Recently, we reported in detail on the microstructure of "214" thin films grown on SLAO.[16] In

Other author information: (Send correspondence to J.W. Seo)
J.W. Seo: E-mail: jwm@zurich.ibm.com;
J.-P. Locquet: E-mail: loc@zurich.ibm.com

In Superconducting and Related Oxides: Physics and Nanoengineering III,
D. Pavuna and I. Bozovic, editors, Proceedings of SPIE Volume 3481 (July 1998)
[0277-786X/98/$10.00]

the present work, we compare the results of the transmission electron microscopy (TEM) investigations of the "214" thin films grown simultaneously on SLAO and STO showing a T_c of 49 and 10 K, respectively. The microstructural properties, particularly the defects present and their types and density, are determined and compared. Furthermore, the lattice deformation was measured based on high-resolution TEM (HRTEM) images and correlated with the spacing between the CuO_2 planes. The results will be discussed with respect to the epitaxial strain and its effect on the increase of T_c.

2. EXPERIMENTAL DETAILS

The Sr-doped "214" thin films were grown in a molecular beam epitaxy (MBE) system equipped with an atomic oxygen source and a reflection high-energy electron diffraction (RHEED) system. The block-by-block deposition technique[17] was used, i.e. a repeated sequence of two layers of (LaSr)O followed by one monolayer of Cu-O and a 10-sec waiting period. Using a recently developed method to determine the lattice parameters from RHEED data,[12] we found that a significant compressive strain can be obtained by using (001)-oriented SLAO substrates and a doping concentration of $x < 0.12$. STO yields tensile strain for all x values.

"214" thin films were grown on SLAO and STO at 750 °C to a final thickness of 15 nm. After the first three monolayers were grown, we allowed an additional waiting period of about 60 sec. The lattice parameters of the film were determined by the in-plane and out-of-plane $\theta - 2\theta$ x-ray diffraction[11] to be

$$a_{\mathrm{Film}} = 3.76 \pm 0.02\,\text{Å} \text{ and } c_{Film} = 13.31 \pm 0.02\,\text{Å} \text{ for SLAO,}$$
$$a_{\mathrm{Film}} = 3.802 \pm 0.02\,\text{Å} \text{ and } c_{Film} = 13.167 \pm 0.02\,\text{Å} \text{ for STO.}$$

The resistivity versus temperature measurement was carried out with a four-point method and is shown in Fig. 1 for both samples[11] together with the data on the bulk compound.[18] The film grown on SLAO has a transition temperature of $T_c = 49.1$ K with a very sharp transition of $\Delta T_c = 0.7$ K. In contrast, the film grown on STO has a T_c of 10 K and a transition of $\Delta T_c = 4$ K. In addition, a typical insulating behavior is observed above T_c, i.e., the resistance increases with decreasing temperature.

For the TEM study, plan-view and cross-section samples were prepared by cutting, grinding and finally thinning the material with an Ar-ion beam until electron transparency is achieved. HRTEM studies were performed in a JEOL 4000EX microscope operated at 400 kV with a point resolution of 0.17 nm, whereas conventional TEM (CTEM) was

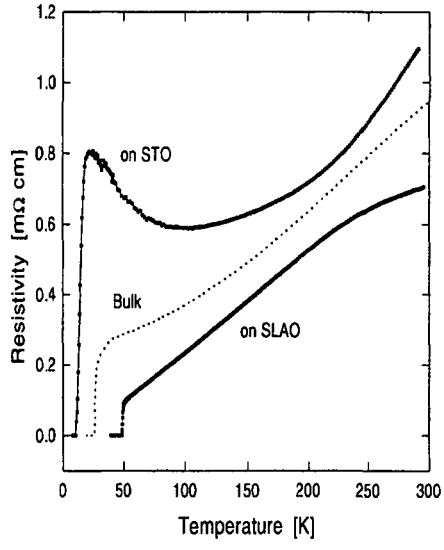

Figure 1. Resistivity versus temperature for "214" grown simultaneously on SLAO and on STO and for the bulk with the same composition. The film on SLAO shows a sharp transition of $\Delta T_c = 0.7$ K; the transition width of the film on STO is $\Delta T_c = 4$ K.

performed with 200 kV microscopes, JEOL 2010 and Philips CM20. Image simulations were made using the Mac Tempas and EMS Stadelman software packages. For lattice image analysis, the HRTEM images were digitized. The lattice displacement was measured using the peak finding process of the SEMPER[19] image processing program and refined with JULIA.[20]

3. RESULTS

3.1. Microstructure of "214" on SLAO

SLAO is tetragonal (I4/mmm) with $a = 3.754$ Å and $c = 12.635$ Å. Its structure is comparable to that of "214": two neighboring (La,Sr)-O planes form a rock-salt structure separated by AlO_2 or CuO_2 layers, as can be seen in the schematic drawing in Fig. 2. A homogeneous epitaxial growth of "214" thin film on this substrate material is obtained, as can be seen in the representative cross-sectional image of the sample in Fig. 3. Here, the full thickness of the film is measured to be 15 nm, which is in agreement with the nominal film thickness derived from the finite-size oscillations of the x-ray diffraction patterns.[6] The epitaxial relationship between the film and the substrate is derived from the diffractogram shown in the inset of Fig. 3:

$$[001]_{Sub}||[001]_{Film} \text{ and } [100]_{Sub}||[100]_{Film}$$

in tetragonal notation. Furthermore, studying the diffractogram more carefully, one finds that the 200 spots of the film and the substrate apparently overlap, whereas the 002 reflections can clearly be distinguished. This indicates a small in-plane mismatch between the film and the substrate, proving that the film is coherent with the substrate. In contrast, the c-axis parameter, which can be derived from the 002 reflections, is about 13.3 Å, which is in agreement with the value determined by x-ray diffraction. However, the film and substrate reveal a characteristic contrast parallel with the interface with a periodic spacing of 6.6 and 6.3 Å, respectively. These can be correlated with the projected image of the 1/2(001) planes in both systems. These characteristic so-called *c/2 fringes* are observed in the film throughout the entire image without any interruption, hence confirming a homogeneous film growth. In particular, these fringes are already present in the vicinity of the interface and interrupted by the substrate surface steps. Thus, homogeneous film growth already takes place from the beginning of the film growth, without amorphous or secondary phases in between. Surface steps of one half-unit cell of SLAO are present, for example in the region marked by an arrow in Fig. 3. Nevertheless, the film shows a perfect continuity without any defects despite, these

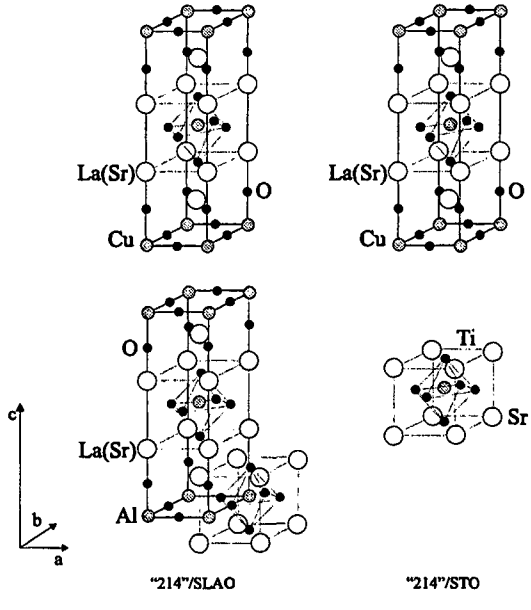

Figure 2. Schematic drawing of the unit cells of "214", SLAO and STO. SLAO has a structure comparable to "214": two neighboring (La,Sr)-O planes form a rock-salt structure separated by AlO_2 or CuO_2 layers.

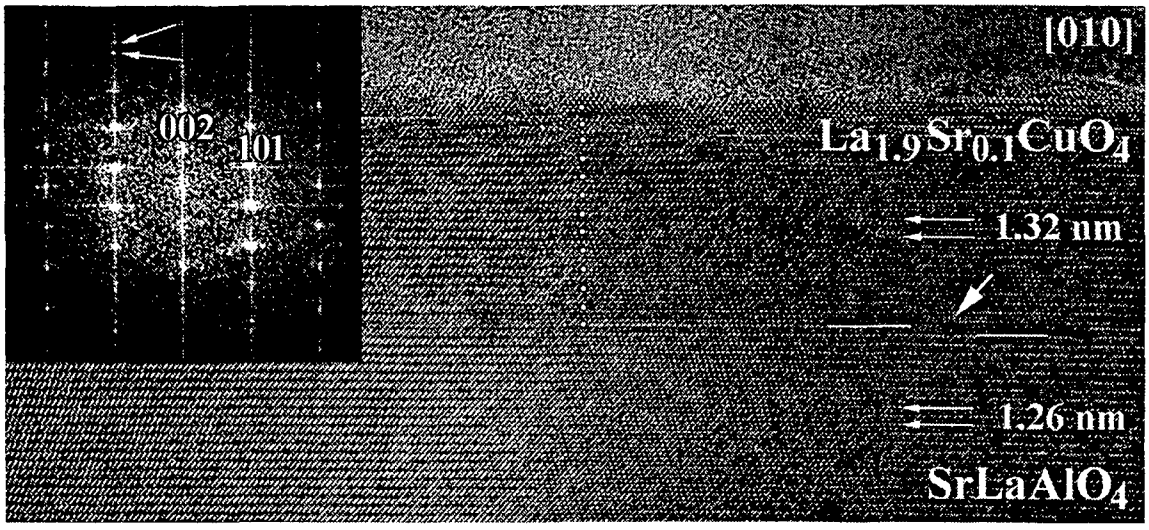

Figure 3. Representative HRTEM image of "214" grown on SLAO in cross section. The film indicates a homogeneous growth; no misfit dislocations are found along the interface. The diffractogram in the inset reveals separated reflections for the film and the substrate along [001]* directions. Along the [100]* direction, the spots apparently overlap, indicating that the in-plane mismatch between "214" and SLAO is very small. The film is 12 unit cells thick, as indicated by the vertical array of dots.

steps. Across the interface, lattice fringes are also in perfect continuity; when looking at the image at grazing incidence parallel to (101) and $(10\bar{1})$, a distortion of the lattice fringes is visible. Nevertheless, no misfit dislocations are observed along the entire interface.

To interpret the HRTEM images properly, image simulations were carried out.[16] A reasonable fit between the calculated and the experimental image was obtained by assuming a specimen thickness of 8 nm and a defocus value of −60 nm. In Fig. 4 an enlarged HRTEM image of the interface is shown including the simulated images. Based on these simulations, the characteristic rows of bright dots in the substrate and the film, which were mentioned above as $c/2$-axis fringes, can be correlated directly with Al and Cu-columns in projection, respectively. The unit cells of SLAO and $La_{1.9}Sr_{0.1}CuO_4$ with the assumed cation positions are indicated in the image. Here, it has to be mentioned that for the present image condition the difference between the pure La- and the La-Sr mixed columns is neglectable. Having identified the Cu columns in the image, the distance between CuO_2 planes in "214" can now be determined by measuring the spacing of the $c/2$-fringes. Accordingly, the CuO_2 spacings averages to 6.645±0.02 Å,[16] yielding 13.29±0.04 Å for the c-axis. The stacking sequence at the interface was determined based on image simulations and can be described as LaO-AlO_2-LaO-CuO_2-LaO; thus, the presence of an intermediate layer of $La(Sr)_2CuAlO_{6-x}$ can be deduced.[16] The simulated image of the interface appears as an inset in Fig. 4.

In Fig. 5(a) the plan-view image of the sample shown was taken in bright-field with of g = 110. Here, dislocation contrasts can be observed that reveal a strain field around the dislocations which are elongated along the ⟨100⟩ and ⟨110⟩ directions. They are irregularly distributed with an average distance of 200 nm. Preferentially, they combine, forming a node of dislocations. By means of extensive CTEM studies, these dislocations were found to be edge-type with Burgers vectors of b = ⟨100⟩ and ⟨110⟩. No other defects, in particular no planar defects, were found. Moiré fringes, which normally indicate an in-plane mismatch between the film and the substrate, are completely missing from the entire sample. Additional selected area diffraction experiments could not distinguish between the spots of the substrate and the film either. This indicates that the in-plane lattice parameter of the film is indeed very close to the substrate value, which is in agreement with the cross-section observations.

3.2. Microstructure of "214" on STO

STO is cubic with $a = 3.905$ Å and yields a tensile strain in the "214" film. A typical plan-view image of the sample is shown in Fig. 5(b) in bright-field mode with g = 110. The epitaxial relationship derived from the diffraction is

Figure 4. Enlarged HRTEM image of the interface including a simulated image. The bright dots of the image contrast can be correlated with Cu and Al columns in "214" and SLAO, respectively. At the interface, a double row of bright dots occurs, which can be explained by an interface stacking sequence of LaO-AlO_2-LaO-CuO_2-LaO leading to an interface structure of $(La,Sr)_2CuAlO_{6-x}$.

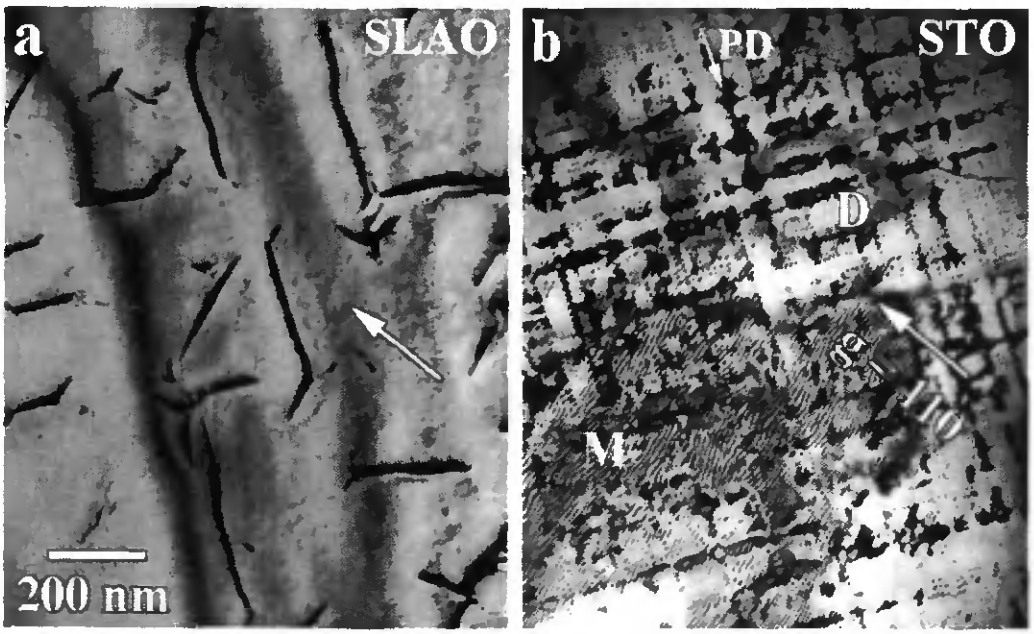

Figure 5. Bright-field image (g = 110) of "214" grown on (a) SLAO and (b) STO in plan view. The SLAO sample indicates a low density of irregularly distributed dislocations. The STO sample contains a periodical array of dislocations (e.g., in the region marked "D") and, additionally, planar faults parallel to ⟨100⟩ directions. Planar defects reveal a broad line contrast, indicating that they are inclined along this viewing direction. One of them is marked by an arrow and "PD".

equivalent to that on SLAO. Moiré fringes are found in the bottom part of the image (marked "M"), indicating that in this part of the TEM specimen the substrate is still present and superimposed with the film. From the distance between the Moiré fringes, the in-plane lattice parameter of the film is found to be about 3.8 Å. This corresponds to a misfit of 2.7%, which was also confirmed by selected-area electron diffraction (SAED) studies. In the top part of the figure, a characteristic contrast of a misfit dislocation network is seen to have an average distance of 16±2 nm. These dislocations were determined with a detailed CTEM study to be edge-type misfit dislocations with a Burgers vector of $\mathbf{b} = \langle 100 \rangle$. Here, it should be emphasized that the dislocations are now connected to a regular network. Besides the dislocations, planar defects are present with an average distance of 155 nm, which can be seen as rather broad lines parallel to the $\langle 100 \rangle$ directions. The broad contrast indicates that their habit planes are inclined; tilting experiments showed that their habit planes are parallel to $\{101\}$ planes.

The cross-sectional view of the sample is presented in Fig. 6. The film indicates a homogeneous epitaxial growth within a small area with a diameter of about 15 nm. Here, the characteristic c-axis fringes (marked by small arrows) are again clearly visible with a well-defined spacing of about $c/2 = 6.6$ Å. At the boundary of these 15-nm regions, planar defects occur, for example in the area indicated by the large arrow. Planar faults were mostly found to be at an inclined angle of about 74° and, occasionally, 50° to the interface. These angles correspond to an inclination angle between the (001) plane and the $\{101\}$ and $\{103\}$ planes, respectively. The distance between the $\{101\}$ and $\{103\}$ planar defects averages 80 and 200 nm, respectively.

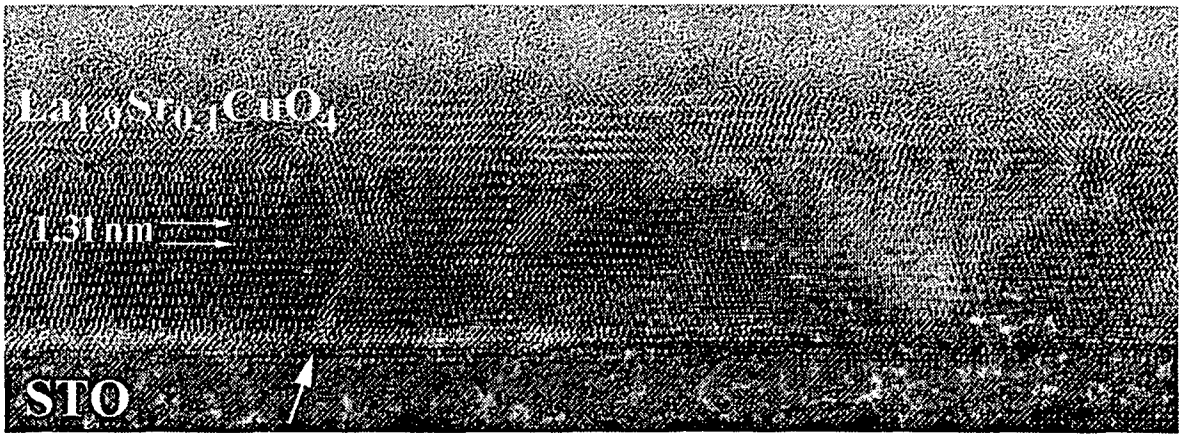

Figure 6. HRTEM image of "214" grown on STO in cross section. The film is not homogeneous, unlike the film on SLAO: it contains planar defects, one of which can be seen in the image and is marked by the large arrow. The planar defects lead to an interruption of CuO_2 planes; this can be seen as an interruption of the c-axis fringes. The film is 12 unit cells thick, as indicated by the vertical array of dots.

At the interface, misfit dislocations are found, which can be seen in Fig. 7 in the enlarged HRTEM image of the interface. Their average distance is about 16 nm; this is in agreement with the value determined by the plan view observation. Furthermore, the interface of this sample indicates a more distorted contrast than the film grown on SLAO (see Fig. 3). Studying the lattice fringes at the interface carefully using lattice image analysis,[20] a 2-nm-wide intermediate layer with an in-plane lattice parameter of about 3.95 Å was found. To interpret the image contrast properly, image simulations were carried out; a reasonable fit was obtained assuming a sample thickness of 6 nm and a defocus value of −70 nm. In Fig. 7 the calculated image was inserted and the "214" structure was confirmed. Based on the direct correlation between the HRTEM image contrast and the cell structure, the average distance between CuO_2 planes was found to be 6.57±0.04 Å, i.e., significantly smaller than the 6.645 Å found for the SLAO sample. A structural model of the interface was developed by assuming an intermediate $(La,Sr)TiO_3$ layer. The calculated image of $STO/(La,Sr)TiO_3$ is inserted in Fig. 7. The large bright dots in the interfacial layer, which have a perovskite-like structure, are in accordance with the contrast in the simulation. A more detailed study of the microstructure of the film will be published elsewhere.[21]

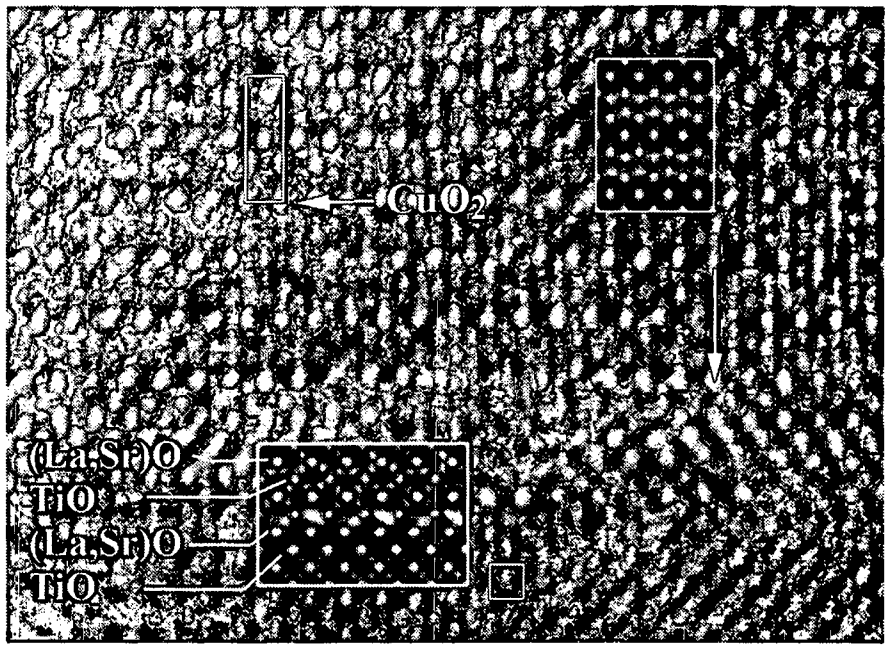

Figure 7. Enlarged HRTEM image of the interface in "214" grown on STO. A misfit dislocation is indicated by an arrow. The interface contains a $(La,Sr)TiO_3$ intermediate layer with a large in-plane parameter than STO. Simulated images are inserted to interpret the image contrast properly; the bright dots can be correlated with cation positions as indicated in the image. The origin of the unit cells are marked by a white rectangle and a square for "214" and STO, respectively.

4. DISCUSSION

For the increase of T_c in "214" thin films, a high amount of compressive strain is essential. In order to compare the amount of strain in both samples, the microstructural properties in both films were studied carefully. In Table 1, the lattice parameters of the various substrate materials are listed, including their misfit compared to the bulk "214" material and the resulting strain in the film. Accordingly, STO has a misfit that is about four times larger than that of SLAO. This explains the large difference in dislocation density between the two films. Recently, Williams *et al.*[10] showed in their TEM study that the microstructure of 98-nm-thin "214" films depends strongly on the substrate material. They observed a difference in the density and types of defects depending on the substrate. In the present

Table 1. Comparison between SLAO and STO leading to compressive and tensile strain in "214", respectively. The lattice parameters measured in these films, compared to the lattice spacing in the equivalent bulk material, indicate an elongation and contraction of the c-axis in SLAO and STO, respectively. The resulting amount of elastic strain is comparable in both samples; only the sign is different. In the STO sample, the high mismatch is already accommodated by the plastic strain, i.e., by the incorporation of the misfit dislocations.

	a_{Sub}, c_{Sub} (Å)	measured a_{Film}, c_{Film} (Å)	misfit $f = \epsilon + \delta$ (%)	elastic strain ϵ (%)	plastic strain δ (%)
Bulk		3.784			
		13.212			
SLAO	3.754	3.76±0.02	0.8	0.63	0.17
	12.635	13.31±0.01		−0.76	
STO	3.905	3.802±0.02	−3.1	−0.54	−2.56
		13.167±0.004		0.35	

study, the difference is more pronounced because we are dealing with ultrathin films. In the case of the film on SLAO, we are apparently close to h_c, therefore only few dislocations were observed. For the film grown on STO, h_c is certainly exceeded, which results in a periodic array of dislocations. To avoid the incorporation of dislocations completely, a thinner film might help. Taking into account that h_c is $\sim f^{-1}$, a film that is 10 to 11 unit cells thick might already be sufficient for SLAO, whereas for an STO thin film only a few unit cells might be required.

Considering the lattice deformation, in the case of SLAO the mismatch is accommodated mainly by the elastic strain. The ratio between the elastic and plastic parts of the strain is about 80% to 20%, whereas for STO the relation is just the opposite, i.e., only 20% of the elastic strain remained. Nevertheless, it has to be noted that the resulting amount of elastic deformation is comparable in both samples (0.63% and −0.54% for SLAO and STO, respectively) despite the different sign of the strain. This almost symmetrical elastic deformation also leads to similar but opposite changes of T_c, +24 K and −15 K.

From the TEM study, we conclude that the "214" thin films grown by MBE have excellent homogeneity. Therefore, one can infer that the strain accommodated by the plastic part is due primarily to the presence of the misfit dislocations and the planar defects. Another important aspect is certainly the intermediate layer as observed in the HRTEM images (Figs. 4 and 7). At the interface of "214"/SLAO, one monolayer of $(La,Sr)_2CuAlO_{6-x}$ was found, which is actually a surprising result considering the structure of "214" and SLAO (see Fig. 2). Owing to the structural similarity, a structure with a continuous stacking of LaO-AlO_2-LaO blocks replacing Al by Cu in the film was initially expected. However, this result shows that the $(La,Sr)_2CuAlO_{6-x}$ structure with two corner-sharing octahedra is favored at the interface.

Recently, the stable phases of the La-Sr-Cu-Al-O system were studied by Wiley *et al.*[22] They successfully grow orthorhombic $LaSrCuAlO_5$ crystals with the lattice parameters of $a = 7.9219$, $b = 11.02$ and $c = 5.4235$ Å. In this structure, Al is surrounded by a tetrahedron of oxygens, whereas Cu is again surrounded by an oxygen octahedron. The relevant orientation of $LaSrCuAlO_5$ for our intermediate layer is [012] with lattice spacings of $d_{(012)} \equiv a^* = 3.8655$ Å and $a/2 \equiv c^* = 3.9645$ Å, which are not in agreement with the parameters derived from our HRTEM image in Fig. 4 ($a = 3.7$ and $c = 4.1$ Å). On the other hand, the interface structure is just one monolayer and certainly heavily strained. In addition, we have to consider that the La and Sr ratio is probably not 1:1 as in the $LaSrCuAlO_5$ structure. Nevertheless, $(La,Sr)_2CuAlO_{6-x}$ is stable at the interface and shows perfect compatibility with SLAO and "214" covering the entire interface, even at a surface step. It has been reported that $LaSrCuAlO_5$ is a semiconductor.[22] Unfortunately, no detailed information exists on the properties of the structure reported here. Properly doped, it could be a superconductor, but in any case it seems to be a good candidate for an intermediate layer in "214" heterostructures. With respect to the lattice deformation, we also conclude that this additional interface structure ($a = 3.7$ Å) gives rise to an increase of the compressive strain in the rest of the film.

In contrast, the interface "214"/STO leads to an intermediate layer of $(La,Sr)TiO_3$, which yields higher tensile strain. The presence of $(La,Sr)TiO_3$ was reported by Werder *et al.*[23] at the interface of "214" on (110)-oriented $SrTiO_3$. On (100)-oriented $SrTiO_3$, they observed no such additional layer. The presence of $(La,Sr)TiO_3$ in our system can be explained by the special growing procedure of the film; after the first three monolayers were deposited, an additional waiting period of about 60 sec was allowed. During this time, interdiffusion of the substrate material might occur, which would favor the formation of such an interface compound. $La_xSr_{1-x}TiO_3$ is a semiconductor in the range of $0.1 \leq x \leq 0.4$ and metallic for $x > 0.4$.[24,25] This system provides again an interesting possibility for the preparation of heterostructures. Nevertheless, the results on both substrates emphasize that for a strain analysis a detailed study of the microstructure is necessary. In addition, the formation of intermediate layers provides an additional parameter to tune the amount of strain.

The fundamental aim of this work is to identify the driving force behind the T_c increase. Based on HRTEM images and image simulations, we can first confirm the presence of a "214" structure and rule out that second phases are responsible for the T_c change. Concerning the defects present, planar faults yield an interruption of the CuO_2 planes and possibly a local change of the stoichiometry[26] along the fault. Therefore, we have to regard such defects as junctions and, probably, this leads to a broad transition.[14,27] Indeed, comparing the two T_c curves in Fig. 1, the transition width is about 6 times larger in the STO sample. The misfit dislocations present have no *c*-axis component and do not affect the atomic structure of "214" film because their Burgers vectors are complete lattice vectors. Therefore, a direct correlation between the misfit dislocations and the change of T_c is not expected. On the other hand, misfit dislocations directly influence the elastic deformation. The lattice parameters derived from x-ray diffraction, SAED patterns and HRTEM images clearly indicate the following lattice deformation: a contraction of

the *ab*-axis and an elongation of the *c*-axis for SLAO and the opposite for STO. In particular, in HRTEM images the lattice deformations are directly correlated with the distance between CuO_2 planes,[16] leading to a larger and smaller CuO_2 spacing for SLAO and STO, respectively, compared to the bulk value. This result shows that the increase of T_c is directly correlated with an increase of the CuO_2 plane distance, i.e., a decoupling of the CuO_2 planes, whereas a stronger coupling leads to a decrease of T_c. This contradicts an existing theory of high-temperature superconductivity, which suggests a higher T_c when the coupling is increased.[28]

ACKNOWLEDGMENTS

We thank L. Rossou and G. Stoffelen for their help in specimen preparation; Ø. Fischer, P. Martinoli, K. Chr. Tillmann, and M. Lentzen for helpful discussions; and the Institut für Festkörperforschung (Forschungszentrum Jülich) for provision of TEM facilities. This work was supported by the Swiss National Science Foundation 2129-42367.94 and the Belgian UIAP 4/10.

REFERENCES

1. L. Gao, Y. Y. Xue, F. Chen, Q. Xiong, R. L. Meng, D. Ramirez, C. W. Chu, J. H. Eggert, and H. K. Mao, "Superconductivity up to 164 K in $HgBa_2Ca_{m-1}Cu_mO_{2m+2+\delta}$ ($m = 1$, 2 and 3) under quasihydrostatic pressures," *Phys. Rev. B* **50**, pp. 4260–4263, 1994.
2. S. L. Bud'ko, J. Guimpel, O. Nakamura, M. B. Maple, and I. K. Schuller, "Uniaxial pressure dependence of the superconducting critical temperature in $RBa_2Cu_3O_{7-\delta}$ high T_c oxides," *Phys. Rev. B* **46**, pp. 1257–1260, 1992.
3. G. L. Belenky, S. M. Green, A. Roytburd, C. J. Lobb, S. J. Hagen, R. L. Greene, M. G. Forrester, and J. Talvacchio, "Effect of stress along the *ab* plane on the J_c and T_c of $YBa_2Cu_3O_7$ thin films," *Phys. Rev. B* **44**, pp. 10117–10120, 1991.
4. H. Sato and M. Naito, "Increase in the superconducting transition temperature by anisotropic strain effect in (001) $La_{1.85}Sr_{0.15}CuO_4$ thin films on $LaSrAlO_4$ substrates," *Physica C* **274**, pp. 221–226, 1997.
5. J.-P. Locquet and E. J. Williams, "Epitaxially induced defects in Sr- and O-doped La_2CuO_4 thin films grown by MBE: implications for transport properties," *Acta Polonica A* **92**, pp. 69–84, 1997.
6. J.-P. Locquet, J. Perret, J. Fompeyrine, E. Mächler, J. W. Seo, and G. V. Tendeloo, "Doubling the critical temperature of $La_{1.9}Sr_{0.1}CuO_4$ using epitaxial strain," *Nature*, 1998, in press.
7. E. A. Fitzgerald, "Dislocations in strained-layer epitaxy: theory, experiment and applications," *Materials Science Reports* **7**, pp. 87–142, 1991.
8. R. People and J. C. Bean, "Calculation of critical layer thickness versus lattice mismatch for Ge_xSi_{1-x}/Si strained layer heterostructures," *Appl. Phys. Lett.* **47**, pp. 322–324, 1985; Erratum, *Appl. Phys. Lett.* **49**, p. 229, 1986.
9. J. W. Matthews and A. E. Blakeslee, "Defects in epitaxial multilayers," *J. Cryst. Growth* **27**, pp. 118–125, 1974.
10. E. J. Williams, A. Daridon, F. Arrouy, J. Perret, Y. Jaccard, J.-P. Locquet, E. Mächler, H. Siegenthaler, P. Martinoli, and Ø. Fischer, "Transmission electron microscopy investigations of defects in molecular beam epitaxy-grown oxide films," *J. Alloys and Comp.* **251**, pp. 11–14, 1997.
11. J. Perret, J. Fompeyrine, J. W. Seo, E. Mächler, Ø. Fischer, P. Martinoli, and J.-P. Locquet, "Critical temperature enhancement by means of substrate induced pressure," *these proceedings.*
12. J.-P. Locquet, Y. Jaccard, A. Cretton, E. J. Williams, F. Arrouy, E. Mächler, T. Schneider, Ø. Fischer, and P. Martinoli, "Variation of the in-plane penetration depth λ_{ab} as a function of doping in $La_{2-x}Sr_xCuO_{4\pm\delta}$ thin films on $SrTiO_3$: implications for the overdoped state," *Phys. Rev. B* **54**, pp. 7481–7488, 1996.
13. D. Dimos, P. Chaudhari, J. Mannhart, and F. K. LeGoues, "Orientation dependence of grain-boundary critical currents in $YBa_2Cu_3O_{7-\delta}$ bicrystals," *Phys. Rev. Lett.* **61**, pp. 219–222, 1988.
14. A. F. Marshall and R. Ramesh, "Microstructure of interfaces in $YBa_2Cu_3O_{7-x}$ thin films," in *Interfaces in High-T_c Superconducting Systems*, S. L. Shindé and D. A. Rudman, eds., pp. 71–115, Springer-Verlag, Berlin, Heidelberg, 1994.
15. J. W. Seo, B. Kabius, U. Dähne, A. Scholen, and K. Urban, "TEM investigation of grain boundaries in $YBa_2Cu_3O_7$ thin films grown on $SrTiO_3$ bicrystal substrates," *Physica C* **245**, pp. 25–35, 1995.
16. J. W. Seo, J. Perret, J. Fompeyrine, G. Van Tendeloo and J.-P. Locquet, "$La_{1.9}Sr_{0.1}CuO_4$ thin films grown under compressive strain: a TEM study," in preparation, 1998.

17. J.-P. Locquet and E. Mächler, "Block-by-block deposition of complex oxide films," *MRS Bulletin* **19**, pp. 39–43, 1994.
18. P. G. Radaelli, D. G. Hinks, A. W. Mitchell, B. A. Hunter, J. L. Wagner, B. Dabrowski, K. G. Vandervoort, H. K. Viswanathan, and J. D. Jorgensen, "Structural and superconducting properties of $La_{2-x}Sr_xCuO_4$ as a function of Sr content," *Phys. Rev. B* **49**, pp. 4163–4175, 1994.
19. O. W. Saxton, T. J. Pitt, and M. M. Horner, "Digital image processing: the Semper system," *Ultramicroscopy* **4**, pp. 343–353, 1979.
20. K. Tillmann, A. Thust, M. Lentzen, P. Swiartek, A. Förster, K. Urban, W. Laufs, D. Gerthsen, T. Remmele, and A. Rosenauer, "Determination of segregation, elastic strain and thin foil relaxation in $In_xGa_{1-x}As$ islands on GaAs(001) by high resolution transmission electron microscopy," *Phil. Mag. Lett.* **74**, pp. 309–315, 1996.
21. J. W. Seo, J. Perret, J. Fompeyrine, and J.-P. Locquet, in preparation, 1998.
22. J. B. Wiley, M. Sabat, S.-J. Hwu, K. R. Poeppelmeier, A. Reller, and T. Williams, "$LaSrCuAlO_5$: A new oxygen-deficient perovskite structure," *J. Solid State Chem.* **87**, pp. 250–260, 1990.
23. D. J. Werder, C. H. Chen, H. L. Kao, and J. Kwo, "Microstructures of thin film $La_{2-x}Sr_xCuO_4$ on $SrTiO_3$ and $LaAlO_3$," *Physica C* **204**, pp. 155–160, 1992.
24. Y. Maeno, S. Awaji, H. Matsumoto, and T. Fujita, "Transport and magnetic properties of $La_xSr_{1-x}TiO_3$," *Physica B* **165-166**, pp. 1185–1186, 1990.
25. Y. Fujishima, Y. Tokura, T. Arima, and S. Uchida, "Optical spectra of titanium oxide perovskites with varying number of d-electrons," *Physica C* **185-189**, pp. 1001–1002, 1991.
26. J. Galy, "(101) and $(\bar{1}01)$ extended defects accounting for the non-stoichiometry of high-T_c superconducting $M_{2\pm\delta}CuO_{4\pm\delta}$ phases ($M_2 = La_{2-x}Sr_x$)," *Acta Cryst.* **B48**, pp. 777–781, 1992.
27. C. L. Jia, H. Soltner, B. Kabius, U. Poppe, K. Urban, and J. Schubert, "A study of antiphase boundaries and "223" planar defects in epitaxial $YBa_2Cu_3O_7$ films by high resolution electron microscopy," *Physica C* **182**, pp. 163–170, 1991.
28. P. W. Anderson, *The Theory of Superconductivity in the High T_c Cuprate Superconductors*, Princeton Univ. Press, Princeton, 1997.